2011

MOVING WALL JET FLOW NEAR CHANNEL EXIT AT MODERATE REYNOLDS NUMBER

Rizwana Amin

MOVING WALL JET FLOW NEAR CHANNEL EXIT AT MODERATE REYNOLDS NUMBER

(Spine title: Moving wall jet flow at moderate Reynolds number)

(Thesis format: Monograph)

by

Rizwana Amin

Graduate Program in Faculty of Engineering

Department of Mechanical and Materials Engineering

2

A thesis submitted in partial fulfillment
of the requirements for the degree of
Master of Engineering Science

The School of Graduate and Postdoctoral Studies
The University of Western Ontario
London, Ontario, Canada

THE UNIVERSITY OF WESTERN ONTARIO
School of Graduate and Postdoctoral Studies

CERTIFICATE OF EXAMINATION

Supervisor	Examiners
Prof. Roger E. Khayat	Prof. El Damatty
	Prof. Liying Jiang
	Prof. P. Kaloni

The thesis by

Rizwana Amin

entitled:

Moving Wall Jet Flow Near Channel Exit at Moderate Reynolds Number

is accepted in partial fulfillment of the
requirements for the degree of
Master of Engineering Science

Date	Chair of the Thesis Examination Board

ABSTRACT

The two-dimensional jet flow of a Newtonian fluid at moderate Reynolds number, emerging from a channel and flowing along one moving plate, while the other plate is stationary, is examined theoretically in this study. In this case, the equations of motion are reduced by expanding the flow field about the basic Couette flow. Inertia is assumed to be large enough, allowing asymptotic development in terms of the inverse Reynolds number. A boundary layer forms adjacent to the free surface, and a classical boundary-layer analysis is applied to find the flow at the free surface and elsewhere. The influence of this boundary layer is investigated by the aid of the method of matched asymptotic expansions. The flow velocity is obtained as composite expansion by matching the flow between the core region and the inner and outer layers. The influence of wall velocity on the shape of the free surface is emphasized. The formulation allows the determination of the steady state flow and free surface profiles analytically, which can serve as boundary condition for computational jet flow further downstream.

Keywords: Couette flow, asymptotic analysis, coating flow.

ACKNOWLEDGEMENT

First and foremost, I praise Allah, the almighty for providing me the opportunity to step in the excellent world of science. This thesis appears in its current form due to the assistance and guidance of several people. I would therefore like to offer my sincere gratitude to all of them.

Dr. Roger E. Khayat, my esteemed supervisor, for his guidance and continuous support during the research. I consider myself very fortunate to have been able to work with him.

Thanks to all of my colleagues in Fluid Mechanics and Polymer processing Research laboratory for making my stay there comfortable and unforgettable.

My parents and my brother, to whom I dedicate my work. I am grateful for their love and best wishes, which despite of their physical absence has helped me in the successful completion of my study in University of Western Ontario.

Finally I am indebted to Md. Abul Kalam Azad, my husband for his constant support and helpful discussions in the study.

TABLE OF CONTENTS

LIST OF FIGURES

LIST OF SYMBOLS

B_4	Constant
c_1	Constant
C_n	Composite expansion operator to $o(\varepsilon^n)$
D	Channel width
E_n	Core expansion operator to $o(\varepsilon^n)$
f_2	Similarity function for the flow in the inner region to $o(\varepsilon^2)$
f_4	Similarity function for the flow in the inner region to $o(\varepsilon^4)$
H_m	Inner expansion operator to $o(\varepsilon^n)$
p	Pressure
p_n	Perturbation pressure to $o(\varepsilon^n)$
Re	Reynolds number
u	Streamwise velocity component
U_n	Perturbation streamwise velocity
w	Transverse velocity component
W_n	Perturbation transverse component
x_∞	Relaxation length
x_m	Distance from the exit where free surface height is maximum
x, y, z	Coordinates
α	Constant
γ	Inverse Reynolds number
δ	Inner layer thickness
ε	Inverse of the cubic root of Reynolds number
ζ	The height of the free surface
ζ_m	Maximum height of the free surface

ξ, η	Coordinates
θ	Similarity variable
μ	Dynamic viscosity
ν	Kinematic viscosity
ρ	Density
σ	Total stress tensor
ϕ	Inclination angle of the free surface
ψ	Stream function
ψ_0	Couette stream function
ψ_n	Stream function perturbation to $o(\varepsilon^n)$

CHAPTER-1

INTRODUCTION

1.1 General introduction

When a real fluid flows along a solid boundary, it will acquire a shear stress at the boundary. While the fluid is detaching itself from a channel or a tube, at the channel exit, the fluid will experience a sudden change in shear stress i.e. the shear stress drops discontinuously from a non-zero value at the wall to zero value on the free surface. This is stress singularity. In any theoretical analysis, stress singularity is the most difficult problem to deal with. However, the computational approach which has prevailed over theoretical analysis for most flow problems, but this is not the case for flows with the singularity. Because, in case of the computational approach, the entire flow field has to be discretized which will incorporate singularity region and then the flow field is difficult to handle numerically if a satisfactory level of accuracy is sought. In this case, asymptotic analysis can be a good alternative which can avoid the singularity.

In the current study, the effect of wall movement on the two-dimensional steady jet of an incompressible fluid near the channel exit at moderately large Reynolds number is examined. The flow configuration corresponds, generically, to a jet inside a channel, flowing or depositing onto a moving wall as it emerges out of the channel i.e. the flow behavior is of Couette type. The basic flow configuration is illustrated schematically in figure 1.1. At the channel exit, the flow will incur singularity.

At large Reynolds number, the upstream diffusion of the stress singularity is small, and the distortion of the original parallel streamlines far upstream is also small. The vorticity generated at the leading edge where the stress singularity occurs diffuses laterally in the normal direction and ultimately contaminates the entire flow field. However, the diffusion is much more significant outside the channel, and is convected downstream, eventually reaching the moving wall.

In the current thesis, the flow near the channel exit is closely examined, and the influence of inertia and wall velocity is emphasized. Inertia is assumed to remain relatively important, allowing the asymptotic development of the flow field in terms of the inverse Reynolds number. As the methodology of asymptotic analysis tends to avoid singularity, the present thesis does not need to deal with singularity.

Asymptotic analyses identify two distinct flow regions: a boundary layer region near the free surface, extending but not including the singular point, and a core region where the flow remains close to fully developed. The inclusion of the singularity is not essential in this case given the similarity character of the flow in the boundary layer region. Note that the boundary layer region extends both upstream and downstream from the singularity. However, although the flow does not remain fully developed as it approaches the exit, the thickness of the boundary layer upstream of the exit is generally small at high Reynolds number, and is often ignored.

Boundary layer theory deals with precisely the asymptotic behavior near the free surface at large Reynolds number. A brief review of the boundary layer theory is given next.

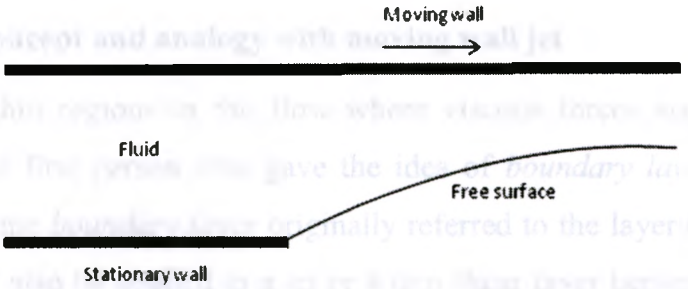

Figure 1.1. Schematic illustration of the basic flow configuration.

1.2 Boundary layer concept and analogy with moving wall jet

Boundary layers are thin regions in the flow where viscous forces are important. L. Prandtl (1904) was the first person who gave the idea of *boundary layer* or *frictional layer*. Although the name *boundary layer* originally referred to the layer of fluid next to the wall, the term may also be applied to a jet or a thin shear layer between two streams of different velocities.

The concept of boundary layer, therefore, implies that flows at high Reynolds numbers can be divided up into two regions: an inviscid flow in the major portion of the flow where viscosity is neglected (this is called inviscid outer flow) and boundary layers near the walls where viscosity must be taken into account. It is seen that the division of the flow field into the inviscid outer flow and the boundary layer leads to considerable simplifications in the theoretical treatment of high Reynolds number flows.

Consider the flow on a plate moving at velocity C. The continuity and Navier–Stokes equations for a two-dimensional steady incompressible flow in Cartesian coordinates are given by

$$\frac{\partial u}{\partial x}+\frac{\partial v}{\partial y}=0 \tag{1.1}$$

$$u\frac{\partial u}{\partial x}+v\frac{\partial u}{\partial y}=-\frac{1}{\rho}\frac{\partial p}{\partial x}+\upsilon\left(\frac{\partial^2 u}{\partial x^2}+\frac{\partial^2 u}{\partial y^2}\right) \tag{1.2}$$

$$u\frac{\partial v}{\partial x}+v\frac{\partial v}{\partial y}=-\frac{1}{\rho}\frac{\partial p}{\partial y}+\upsilon\left(\frac{\partial^2 v}{\partial x^2}+\frac{\partial^2 v}{\partial y^2}\right) \tag{1.3}$$

where u and v are the velocity components in the x and y directions, respectively, ρ is the density, p is the pressure, and ν is the kinematic viscosity of the fluid at a point. Thus, u and v are the streamwise and transverse (wall normal) velocities, respectively, inside the boundary layer. Using the usual scaling analysis, it can be shown that the above equations of motion reduce within the boundary layer to become

$$\frac{\partial u}{\partial x}+\frac{\partial v}{\partial y}=0 \tag{1.4}$$

$$u\frac{\partial u}{\partial x}+v\frac{\partial u}{\partial y}=-\frac{1}{\rho}\frac{\partial p}{\partial x}+\upsilon\frac{\partial^2 u}{\partial y^2} \tag{1.5}$$

$$\frac{\partial p}{\partial y}=0 \tag{1.6}$$

The asymptotic analysis also shows that v, the transverse velocity, is small compared to u, the streamwise velocity, and that variations in flow in the streamwise direction are generally much lower than those in the transverse direction. Since the static pressure p is independent of y, then pressure at the edge of the boundary layer is the pressure throughout the boundary layer at a given streamwise position. The external pressure may be obtained through an application of Bernoulli's equation. Let U be the fluid velocity outside the boundary layer, where u and U are both parallel. Note that U is different than the moving plate velocity. This gives upon substituting for p the following result

$$u\frac{\partial u}{\partial x}+v\frac{\partial u}{\partial y}=U\frac{\partial U}{\partial x}+\upsilon\frac{\partial^2 u}{\partial y^2} \tag{1.7}$$

For a flow in which the static pressure p also does not change in the direction of the flow then

$$\frac{dp}{dx}=0 \tag{1.8}$$

Therefore, the equation of motion simplifies to become

$$u\frac{\partial u}{\partial x}+v\frac{\partial u}{\partial y}=\upsilon\frac{\partial^2 u}{\partial y^2} \tag{1.9}$$

The above analysis is for any instantaneous laminar or turbulent boundary layer, but is used mainly in laminar flow studies.

For a flat plate the boundary conditions are the following:

At y=0(wall): u=C, v=0 (no slip),

At $y=\delta(x)$: u=U(x). (1.10)

Of closer relevance to the current moving wall jet problem is the situation where the flow far from the moving plate is at rest. In this case, U = 0. The next step is to find the similarity solution for the boundary layer equations. A similarity solution is a form of solution in which at least one co-ordinate lacks a distinguished origin; more physically, it describes a flow which 'looks the same' either at all times, or at all length scales. Following Blasius, using co-ordinate transformation, the dimensionless velocity profile u/C is taken as a function of η:

$$\frac{u}{C} = f'(\eta) \qquad \eta = y\left(\frac{C}{\nu x}\right)^{1/2} \tag{1.11}$$

Substituting (1.11) into (1.9) the nonlinear PDE changes to third-order nonlinear ODE for f, namely

$$f''' + \frac{1}{2} f f'' = 0 \tag{1.12}$$

with the boundary conditions

At $\eta = 0$: $f = 0$, $f' = 1$; $\eta \to \infty$: $f' = 0$.

This problem is described briefly in Schlichting (2000) and more elaborately by Sakiadis (1961).

The typical configuration of a wall jet is shown in figure 1.2, which illustrates the analogy between the current problem and boundary layer at a moving plate of Schlichting (2000).

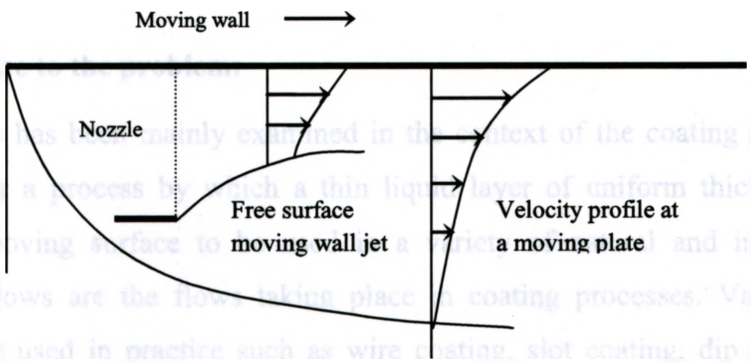

Figure 1.2: Analogy between current problem and boundary layer at moving plate.

1.3 Practical relevance to the problem:

Moving wall jet flow has been mainly examined in the context of the coating process. Coating is defined as a process by which a thin liquid layer of uniform thickness is applied to a fixed/moving surface to be used in a variety of natural and industrial processes. Coating flows are the flows taking place in coating processes. Variety of coating processes are used in practice such as wire coating, slot coating, dip coating, knife coating, roll coating etc.

Wire coating by extrusion is a continuous process practiced primarily in the manufacturing of wires and cables. A schematic representation of a coating die is shown in figure 1.3(a). Quoting Mitsoulis (1986), "The bare wire is introduced into the rear of a cross-head die and travels through the mandrel and guider tip. The polymer melt is extruded around the wire to form a coating surface." In a dip-coating process, "a substrate is dipped into a liquid coating solution and then is withdrawn from the solution at a controlled speed. Coating thickness generally increases with faster withdrawal speed. The thickness is determined by the balance of forces at the stagnation point on the liquid surface. A faster withdrawal speed pulls more fluid up onto the surface of the substrate before it has time to flow back down into the solution. The thickness is primarily affected by fluid viscosity, fluid density, and surface tension." *(http://www.ytca.com/dip_coating)*

In the slot die process *(http://www.tciinc.com/coating.html)*, the coating is squeezed out by gravity or under pressure through a slot and onto the substrate. If the coating is 100% solid, the process is termed 'extrusion' and in this case, the line speed is frequently much faster than the speed of the extrusion. This enables coatings to be considerably thinner than the width of the slot. In slot coating process, if the pressure is negligible during the coating flow coming out, the idea can be relevant to the current problem.

Finally, knife coating is a process which relies on a coating being applied to the substrate which then passes through a 'gap' between a 'knife' and a support roller. As the coating and substrate pass through, the excess is scraped off. This process can be used for high viscosity coatings and very high coat weights, such as plastisols and rubber coatings.

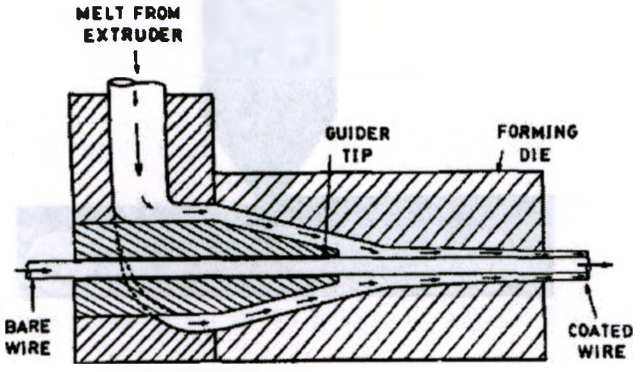
MELT FROM
EXTRUDER
GUIDER
TIP
FORMING
DIE
BARE
WIRE
COATED
WIRE

(a)

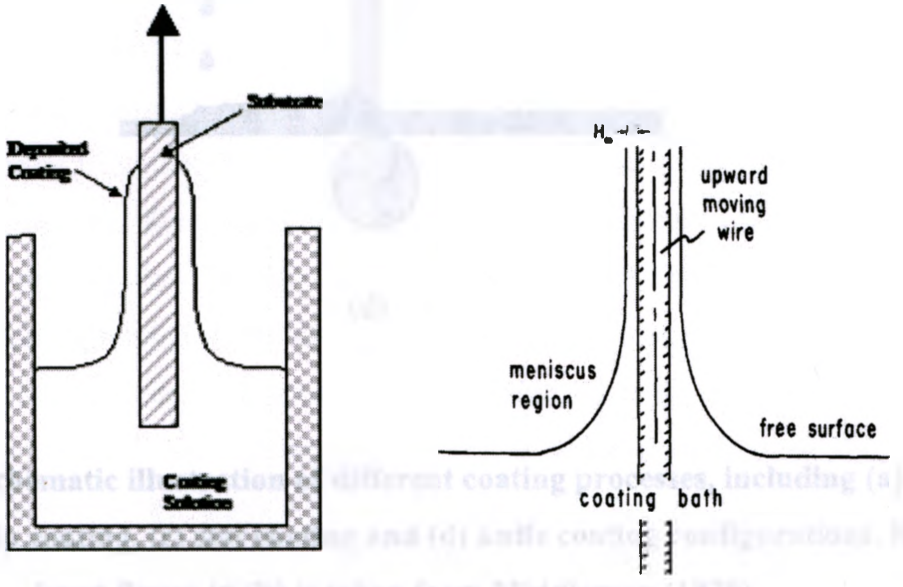
Substrate
Deposited
Coating
Coating
Solution
upward
moving
wire
meniscus
region
free surface
coating bath

(b)

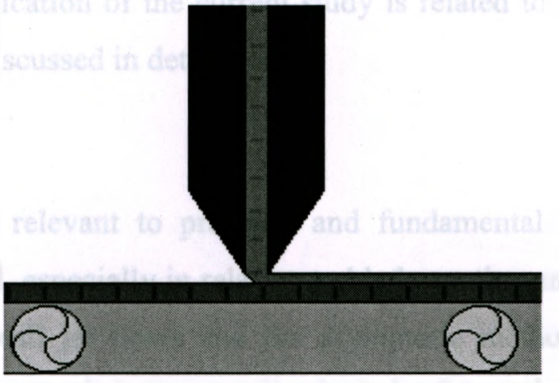

(c)

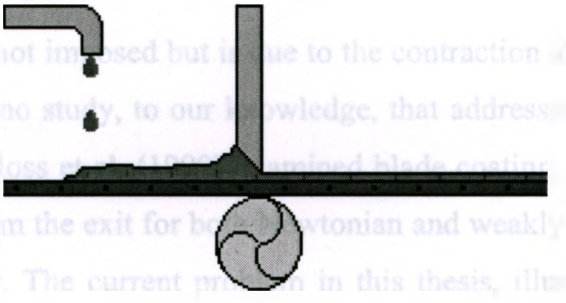

(d)

Figure 1.3: Schematic illustration of different coating processes, including (a) wire coating, (b) dip coating, (c) slot coating and (d) knife coating configurations. Right-hand figure in (b) is taken form Middleman (1978)

Perhaps the closest application of the current study is related to blade coating and wire coating, which will be discussed in detail below.

1.4 Literature review

In this section, studies relevant to practical and fundamental aspects of the current problem will be reported, especially in relation to blade coating and wire coating, as well as studies on moving wall jet flows and the asymptotic methodologies. A schematic illustration of the blade coating process is given in figure 1.4. Blade coating flow configuration represents flow in the narrow nonuniform channel formed between a fixed blade of prescribed shape and a plane substrate moving parallel to itself. Typically, and as the figure shows, blade coating involves the movement of the substrate as well as the action of a pressure gradient, which are both responsible for the flow.

The driving pressure is not imposed but is due to the contraction ahead of the exit (figure 1.4). However, there is no study, to our knowledge, that addresses the flow downstream from the channel exit. Ross et al. (1999) examined blade coating, but limited their study to the flow upstream from the exit for both Newtonian and weakly non-Newtonian fluids, using lubrication theory. The current problem in this thesis, illustrated in figure 1.1, is related to blade coating flow. In fact, if the contraction upstream from the exit is not severe, or the straight section of the channel in figure 1.4 is long, then the action of the driving pressure becomes negligible near the exit compared to the action of the moving substrate. In this case, the flow upstream of the exit is of the Couette type. This will be the assumption in the current thesis which is not unrealistic. Indeed, figure 1.5 illustrates the flow behavior near and upstream from the tube exit in the case of wire coating. In this case, the Couette flow is clearly evident near the exit. Note that figure 1.5 can be regarded as a magnification of the flow near the exit in figure 1.3a.

Extensive literature can be found on wire coating flows involving both Newtonian and viscoelastic liquids. However, as in the case of blade coating, most of the studies in wire coating also focused on the flow upstream from the die exit and not on the shape of the actual coat. Some exceptions can be noted. Middleman (1978) examined high speed wire coating by withdrawal from a bath of viscoelastic liquid. In his work, the thickness of

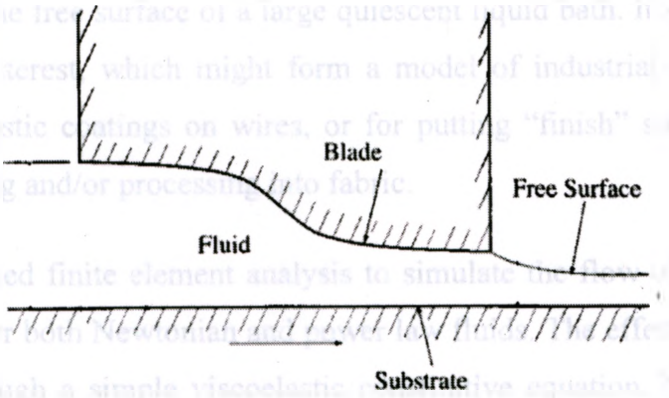

Figure 1.4: Schematic illustration of blade coating flow (from Ross et al. 1999).

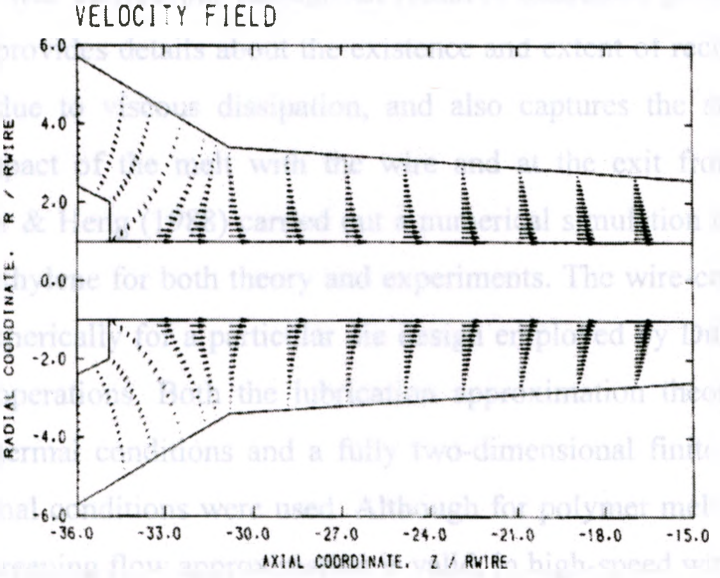

Figure 1.5: Typical velocity profile development obtained from the non-isothermal analysis in numerical analysis of wire coating.(from Mitsoulis et al 1988)

liquid coating is concerned which can be entrained by a wire or filament withdrawn vertically through the free surface of a large quiescent liquid bath. It showed the features of the system of interest, which might form a model of industrial systems for use in producing solid plastic coatings on wires, or for putting "finish" solutions onto textile fibers prior to dyeing and/or processing into fabric.

Mitsoulis (1986) used finite element analysis to simulate the flow of polymers through wire-coating dies for both Newtonian and power law fluids. The effect of normal stresses was examined through a simple viscoelastic constitutive equation. Nonisothermal wire coating was studied to obtain the temperature field within the melt. The effect of a slip condition at the solid boundaries was also examined. The determination of the coating melt free surface was carried out through an iterative numerical procedure. The finite element solution provides details about the existence and extent of recirculation regions, about hot spots due to viscous dissipation, and also captures the stress singularities present at the impact of the melt with the wire and at the exit from the die. Later, Mitsoulis, Wagner & Heng (1988) carried out a numerical simulation of wire-coating of low-density polyethylene for both theory and experiments. The wire-coating process has been analyzed numerically for a particular die design employed by DuPont Co. in high-speed industrial operations. Both the lubrication approximation theory for power-law fluids under isothermal conditions and a fully two-dimensional finite element analysis under nonisothermal conditions were used. Although for polymer melt flows in general, $Re << 1$ and the creeping flow approximation is valid, in high-speed wire coating Re may be as high as 10 and the inertia terms should be included.

From a more fundamental perspective, as mentioned earlier, the current problem is closely related to the laminar boundary-layer flow on a moving continuous flat surface. This problem was investigated early by Sakiadis (1961), who adopted two methods to obtain the flow profile. One method involves the numerical determination of the similarity solution of the boundary-layer equations and the other is an integral method, based on an assumed velocity profile that satisfies the appropriate boundary conditions. Good agreement was obtained between the results of these two methods of solution (see

also Schlichtling 2000). The literature on wall jet flow along a moving wall is limited in comparison to the stationary wall jet problem. The wall jet is created when fluid is discharged from a slot and spreads along a plate. This kind of flow along a stationary plate and in a stagnant fluid was investigated early by Glauert (1956) who gave a similarity solution. A complete analysis of this flow can be found in the textbook of Schlichting and Gersten (2000)and a good review is presented by Magyari and Weidman (2006). Therefore a lot of studies on wall jet of different shapes of nozzles or walls have been reported. On the other hand, the flow patterns of two dimensional wall jet when the wall is moving have not been ascertained. This is in fact one of the motives behind the present study. A flow field formed by a moving flat plate and a two dimensional wall jet running parallel to it was experimentally studied by Maki (1983). Mahmood (1987) considered a laminar wall jet from a momentum source at the leading edge on a wall which is moving in the same direction with uniform velocity. For small distance along the wall a solution was found by using a natural coordinate expansion in powers of $x^{1/2}$. For large distance, the asymptotic solution is approached and then he applied a numerical solution to join two coordinate expansions. More recently, the flow of a laminar wall jet along a moving plate was also considered by Pantokratoras (2010). The governing boundary-layer equations are converted into non-dimensional form and are solved numerically. However, an interesting observation from the paper is that the correct velocity profile is obtained when less step size is used and this profile is similar to current thesis. It was found that as x increases the influence of the moving wall increases and the maximum velocity approaches the plate which supports the current analysis.

The rest of this section comprises the literature survey from the point of view of the methodology i.e. asymptotic analysis used to solve the current problem. Asymptotic analysis has been successfully adopted for flows in the visco-capillary range (Goren & Wronski 1966, Ruschak & Scriven 1977, Higgins 1982) and, more closely to the present problem, in the visco-inertial range (Tillett 1968, Philippe & Dumargue 1991). In this regard, however, little focus has been on jet flow taking inertia into account. Tillett (1968) analyzed the moderately inertial laminar free jet flow near the channel exit using the method of matched asymptotic expansions. Tillett was able to obtain the asymptotic contraction ratio of the jet far downstream using an integral analysis. The results were in

good agreement with the experimental results found by Middleman & Gavis (1961). Consequently, the method of matched asymptotic analysis proved to be a very successful tool in examining the flow structure of the jet near the channel exit. Miyake et al (1979) carried out a similar analysis on a vertical jet of inviscid fluid taking into account gravity effect. They considered far downstream flow regions to match with 'near-exit' flow and thus extended the validity of the methodology described by Tillett (1968) to the far downstream region from the exit. Philippe & Dumargue (1991) also applied a similar analysis to Tillett's for viscous axisymmetric vertical jets, emphasizing the interplay between the effects of gravity and inertia on the free surface shape and the velocity profile. A local similarity transformation was carried out by Wilson (1985) for the axisymmetric viscous-gravity jet of the boundary layer type flow close to the free surface. Asymptotic analyses have also been successfully implemented for non-Newtonian flows. See, for instance, the work of Denier & Dabrowski (2004) on boundary layer flow, and the work of Zhao & Khayat (2007) for the spreading of a liquid jet.

Free surface and interfacial flows are inherently complicated because of the unknown position of the surface or interface. The presence of the stress singularity adds considerably to the complexity of the problem and solution. Both analytical and computational solution methodologies have been pursued in the literature. A combination of analytical and numerical treatments has also been proposed (Shi, Breuer & Durst 2004). As mentioned earlier, in a computational approach, the entire flow domain must be discretized, including the singularity and its surrounding region, both upstream and downstream from the exit. Higher accuracy is achieved through mesh refinement, which captures more effectively the singularity but leads simultaneously to the presence of stronger flow gradients that are difficult to handle numerically (Pasquali & Scriven 2002). In order to circumvent the difficulty with the unknown free surface, Tsukiji & Takahashi (1987) wrote the flow equations in a curvilinear coordinate system related to the network comprising the streamlines and their orthogonal trajectories. Although this approach simplifies the implementation of the boundary conditions, it complicates the flow equations.

1.5 Concluding remarks

In conclusion, most of the studies in the literature assumed negligible Reynolds number and emphasized the relation between the properties of the coating fluid and the interfacial behaviour of the coating layer. The present study attempts to examine the blade coating flow at moderate Reynolds number, well below the transition regime which corresponds approximately to Re = 1500 for channel flow. Correlations of surface properties are obtained in terms of the wall velocity and inertia so that better control can be achieved in a coating process to obtain desired level of coating thickness. The method of matched asymptotic expansions is used to obtain the flow near the free surface (inner layer) and in the core region.

CHAPTER-2

GENERAL PROBLEM AND BOUNDARY LAYER FLOW NEAR THE FREE SURFACE

2.1 Governing equations

Consider the two-dimensional flow of an incompressible fluid of density ρ and viscosity μ, emerging from a channel of width D. The flow configuration is schematically depicted in figure 2.1 in the (X, Z) plane. The X axis is taken along the stationary wall and the Z axis is chosen in the transverse direction across the channel. The channel exit coincides with X = 0. The flow is induced by translation of upper wall, moving at velocity C. The stream function of the basic Couette flow is obtained from

$$\Psi = \frac{C}{D}\frac{z^2}{2} \tag{2.1}$$

Non-dimensional variables are introduced by measuring lengths with respect to D and stream function with respect to CD. In this case, the Reynolds number, Re, is given by

$$\mathrm{Re} = \frac{DC}{\nu} \tag{2.2}$$

where ν is the kinematic viscosity. Now, (2.1) will turn out to be the leading order solution in the core region, and is conveniently introduced here as

$$\psi_0 = \frac{{z_0}^2}{2} \tag{2.3}$$

In this study, Re is assumed to be moderately large. The non-dimensional conservation of momentum equation for the laminar steady flow takes the following form

$$\psi_z\psi_{xz} - \psi_x\psi_{zz} = -p_x + \frac{1}{\mathrm{Re}}\left(\psi_{xxz} + \psi_{zzz}\right) \tag{2.4a}$$

$$-\psi_z\psi_{xx} + \psi_x\psi_{xz} = -p_z - \frac{1}{Re}\left(\psi_{xxx} + \psi_{xzz}\right) \qquad (2.4b)$$

2.2 Kinematic and Dynamic boundary conditions

Kinematic boundary condition implies that there is no component of velocity in the transverse direction. In other words there is no flow across the free surface i.e. kinematic boundary condition is a no penetration condition. If the tangential velocity component is $\vec{v}$, then the component of velocity in the normal direction $\vec{v}.\vec{n} = 0$

Kinematic condition also means that free surface is itself a streamline. Therefore,

$$w = \frac{dh}{dt} = \frac{\partial h}{\partial t} + \frac{\partial h}{\partial x}\frac{\partial x}{\partial t} = uh_x$$

In terms of stream function, the above equation can be written as follows

$$\frac{\partial \psi}{\partial x} + \frac{\partial \psi}{\partial z}\frac{\partial h}{\partial x} = 0 \qquad (a)$$

From the chain rule, we know that,

$$d\psi = \frac{\partial \psi}{\partial x}dx + \frac{\partial \psi}{\partial z}dz$$

Now differentiating $d\psi$ with respect to x,

$$\frac{d\psi}{dx} = \frac{\partial \psi}{\partial x} + \frac{\partial \psi}{\partial z}\frac{dz}{dx}$$

On the free surface z = h(x). Therefore we can write,

$$\frac{d\psi}{dx} = \frac{\partial \psi}{\partial x} + \frac{\partial \psi}{\partial z}\frac{dh}{dx} \qquad (b)$$

From equation (a) and (b), it can be concluded that $d\psi = 0$, or $\psi = \text{constant}$.

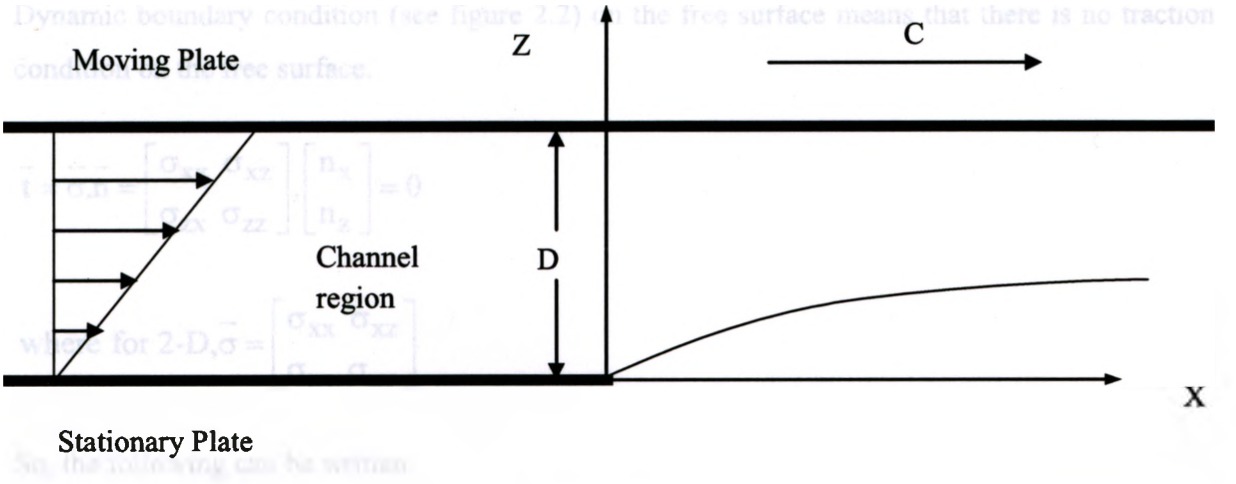

Figure 2.1: Schematic illustration of the 2D moving wall jet flow. Note that the all notations are dimensional.

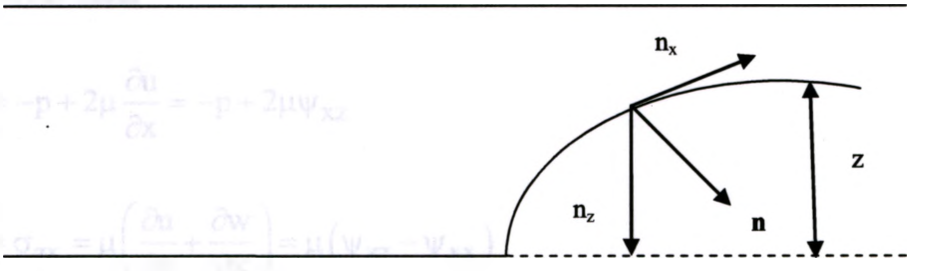

Figure 2.2: Schematic illustration of dynamic boundary condition

Dynamic boundary condition (see figure 2.2) on the free surface means that there is no traction condition on the free surface.

$$\vec{t} = \vec{\vec{\sigma}}.\vec{n} = \begin{bmatrix} \sigma_{xx} & \sigma_{xz} \\ \sigma_{zx} & \sigma_{zz} \end{bmatrix} . \begin{bmatrix} n_x \\ n_z \end{bmatrix} = 0$$

where for 2-D, $\vec{\vec{\sigma}} = \begin{bmatrix} \sigma_{xx} & \sigma_{xz} \\ \sigma_{zx} & \sigma_{zz} \end{bmatrix}$

So, the following can be written

$$\sigma_{xx} n_x + \sigma_{xz} n_z = 0 \qquad (c)$$

$$\sigma_{zx} n_x + \sigma_{zz} n_z = 0 \qquad (d)$$

For viscous fluid,

$$\sigma_{xx} = -p + 2\mu \frac{\partial u}{\partial x} = -p + 2\mu\psi_{xz}$$

$$\sigma_{xz} = \sigma_{zx} = \mu\left(\frac{\partial u}{\partial z} + \frac{\partial w}{\partial x}\right) = \mu\left(\psi_{zz} - \psi_{xx}\right)$$

$$\sigma_{zz} = -p + 2\mu \frac{\partial w}{\partial z} = -p - 2\mu\psi_{zx}$$

Now, components of normal $\vec{n}$ are

$$n_x = \frac{-\zeta'}{\sqrt{\zeta'^2 + 1}} \text{ and } n_z = \frac{1}{\sqrt{\zeta'^2 + 1}}$$

So equation (c) and (d) read

$$-\zeta'\left(-p + 2\mu\psi_{xz}\right) + \mu\left(\psi_{zz} - \psi_{xx}\right) = 0$$

$$\mu\left(\psi_{zz} - \psi_{xx}\right)\left(-\zeta'\right) + \left(-p - 2\mu\psi_{xz}\right) = 0$$

Finally, we can say that for $x > 0$, the kinematic and dynamic boundary conditions at the free surface, $z = \zeta(x)$, are as follows

$$\psi(x, z = \zeta) = 0 \tag{2.5a}$$

$$p + \frac{1}{Re}\left[2\psi_{xz} + \zeta'(\psi_{zz} - \psi_{xx})\right] = 0 \tag{2.5b}$$

$$p\zeta' - \frac{1}{Re}(2\psi_{xz}\zeta' - \psi_{zz} + \psi_{xx}) = 0 \tag{2.5c}$$

A prime denotes total differentiation. Inside the channel ($x < 0$), the following conditions must be satisfied, namely,

$$\psi_z = 1 \quad \psi_x = 0 \quad \text{at } z=1 \tag{2.6a}$$

$$\psi_z = 0 \quad \text{at } z=0 \tag{2.6b}$$

$$\psi \to \frac{z^2}{2} \text{ as } x \to -\infty \tag{2.6c}$$

The flow is supposed to have the basic Couette profile (2.3) to lowest order and is modified when the fluid leaves the channel in the form of the wall jet. Quoting Tillett (1968), "when the fluid detaches itself from the wall of the channel, the removal of the wall stress causes a boundary layer to form in a region near the free surface. In this region, the linear velocity profile adjusts itself so as to satisfy the condition of zero traction at the free surface. In the inviscid limit, this condition would not be imposed since there is no (viscous) mechanism for the stress singularity to diffuse, and all the conditions of the problem would be satisfied by postulating that the linear profile continues unchanged in the jet region. However, no uniqueness theorem exists for this inviscid problem, and it is conceivable that other solutions might exist." Nevertheless, it is assumed in this paper that the fully developed Couette flow is everywhere the proper inviscid limit. "With this assumption, the flow in the core of the jet is, to lowest order, not affected by the flow in the boundary layer region" near the free surface although the boundary layer is expected to induce perturbations to the basic Couette flow, when higher order terms are included, both for

the flow upstream and downstream from the channel exit. This assumption is similar to the one made by Smith (1979) for the tube flow with severe constriction, where the flow field in the core region, to leading order, satisfy the inviscid equations of motion.

Figure 2.3 illustrates schematically the different flow regions for the moving wall jet. In each region, different physical mechanisms dominate the flow with corresponding characteristic length scales. In particular, for the flow outside the channel, the region close to the free surface, the *inner* region, is shear dominated and the flow is of the boundary layer type. In between the inner region and the moving wall, the *core* region, both shear ($\frac{\partial u}{\partial z}$) and elongation ($\frac{\partial u}{\partial x}$) prevail as a result of the high proportion of the Couette character of the flow and the contracting jet. The core region also extends upstream from the exit. At the channel exit, $x = 0$, the shear stress undergoes a step change from a non-zero value (of dimensionless value 1) at the lower wall, $z = 0$, to zero at the free surface, $z = \zeta(x)$. The effect of this drop diffuses upstream inside the channel ($x < 0$) over a distance x_0 where fully developed Couette flow is recovered, and downstream ($x > 0$) toward the moving wall over a distance x_∞, at which point the flow is entirely of the boundary layer type. The current study is concerned with the flow outside the channel where the similarity solution in the inner region is matched onto the core solution. This core solution is then matched with the core solution inside the channel at the channel exit. Another layer also exists close to the upper wall which is denoted as the *outer* layer as shown in figure. It is important to observe that no matching is required for the similarity solution in the streamwise direction, and the flow singularity at the origin is entirely avoided in the solution process. This results in a major advantage of the current formulation compared to alternative solution methods. The problem is now examined by considering separately the flow near the free surface (inner region), the flow in the core region, and the flow in the vicinity of the moving wall (outer region). The composite flow is obtained upon matching the solutions at the interface between the two regions. Part of the formulation in each layer is similar to the free jet formulation carried out by Tillett (1968).

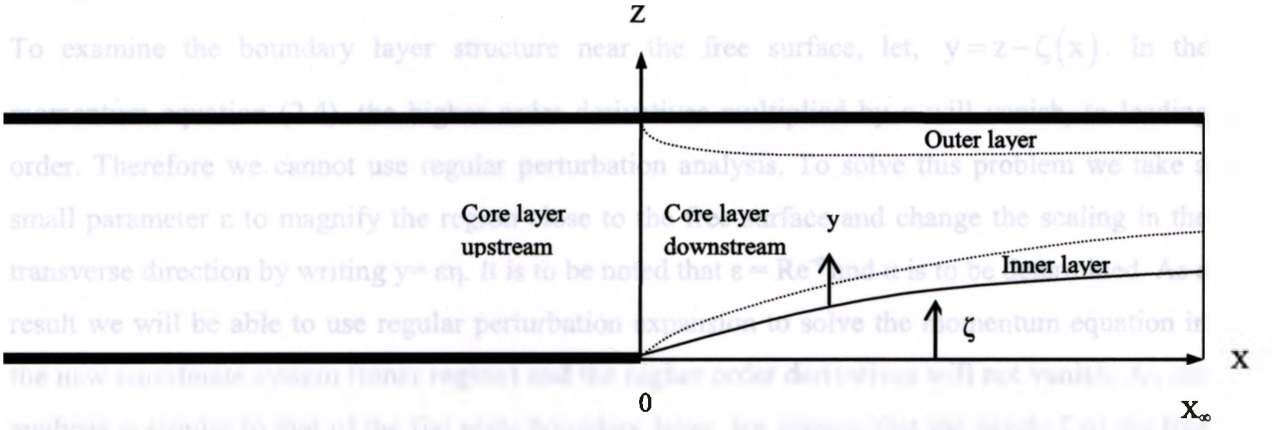

Figure 2.3: Schematic illustration of the computational domain, including the inner, outer and core regions. All notations are dimensionless.

2.3 The flow in the inner layer close to the free surface

To examine the boundary layer structure near the free surface, let, $y = z - \zeta(x)$. In the momentum equation (2.4), the higher order derivatives multiplied by ε will vanish, to leading order. Therefore we cannot use regular perturbation analysis. To solve this problem we take a small parameter ε to magnify the region close to the free surface and change the scaling in the transverse direction by writing $y = \varepsilon\eta$. It is to be noted that $\varepsilon = Re^{-\alpha}$ and α is to be determined. As a result we will be able to use regular perturbation expansion to solve the momentum equation in the new coordinate system (inner region) and the higher order derivatives will not vanish. As our analysis is similar to that of the flat plate boundary layer, we assume that the height ζ of the free surface is of the same order of magnitude as the boundary layer thickness, and write $\zeta(x) = \varepsilon h(x)$, and henceforth work with h. In this case, $h(x) = O(1)$ as $\varepsilon \to 0$, i.e. ζ tends to 0 with ε. In the matching process, in chapter 3, it will be shown that $h = O(1)$ indeed. Following Tillett (1968), the following change of coordinates is introduced, namely,

$$x = \xi, \qquad z = \varepsilon(\eta + h) \tag{2.7}$$

in (2.4a) and (2.4b), it is concluded that

$$\psi_\eta\psi_{\xi\eta} - \psi_\xi\psi_{\eta\eta} = -\varepsilon^2\left(p_\xi - h'p_\eta\right) + \varepsilon^{\left(\frac{1}{\alpha}-1\right)}\psi_{\eta\eta\eta} + \varepsilon^{\left(\frac{1}{\alpha}+1\right)}\left(\psi_{\xi\xi\eta} - h''\psi_{\eta\eta} - 2h'\psi_{\xi\eta\eta} + h'^2\psi_{\eta\eta\eta}\right) \tag{2.8a}$$

$$-\psi_\eta\psi_{\xi\xi} + \psi_\xi\psi_{\xi\eta} + h''\psi_\eta^2 + h'\left(\psi_\eta\psi_{\xi\eta} - \psi_\xi\psi_{\eta\eta}\right) = -p_\eta - \varepsilon^{\left(\frac{1}{\alpha}-1\right)}\left(\psi_{\xi\eta\eta} - h'\psi_{\eta\eta\eta}\right) - \varepsilon^{\left(\frac{1}{\alpha}+1\right)}\left(\frac{\partial}{\partial\xi} - h'\frac{\partial}{\partial\eta}\right)^3\psi \tag{2.8b}$$

The aim is to find a solution of the transformed equations of (2.4) in the form of an "inner expansion" in ε. In order to match this to the core Couette flow, it is necessary to have $\psi \sim y^2$ as $\eta \rightarrow \infty$ in the inner region, to lowest order in ε. Therefore, ψ must be of order ε^2. Similarly to jet flow (Tillett 1968), the value of α is determined by requiring that the convective and viscous terms balance, leading to $\alpha = 1/3$.

Actually, there is another possibility for the value of alpha which is 1. For this value of α, it shows that to the lowest order, the inertia becomes negligible and the flow acts as creeping flow and the convective and viscous terms balance are observed only for higher order terms. The streamwise and depthwise velocity components, u and w, respectively, are now expressed in terms of the stream function as

$$u = \psi_z = \frac{1}{\varepsilon}\psi_\eta \tag{2.9a}$$

$$w = -\psi_x = -\psi_\xi + h'\psi_\eta \tag{2.9b}$$

From (2.9a), it is obvious that u is of order ε. Considering the fact that u in the inner region must match the velocity in the core region: $u \rightarrow z$, it is also inferred that u must be of order ε inside the inner region. The order of w can be found using the continuity equation when written in terms of inner variables, or

$$\varepsilon u_\xi - \varepsilon h' u_\eta + w_\eta = 0 \tag{2.10}$$

Thus, w is of order ε^2. The momentum conservation equations can be re-written as

$$\begin{aligned}\psi_\eta\psi_{\xi\eta} - \psi_\xi\psi_{\eta\eta} &= -\varepsilon^2\left(p_\xi - h'p_\eta\right) + \varepsilon^2\psi_{\eta\eta\eta} \\ &+\varepsilon^4\left(\psi_{\xi\xi\eta} - h''\psi_{\eta\eta} - 2h'\psi_{\xi\eta\eta} + h'^2\psi_{\eta\eta\eta}\right)\end{aligned} \tag{2.11a}$$

$$\begin{aligned}-\psi_\eta\psi_{\xi\xi} + \psi_\xi\psi_{\xi\eta} + h''\psi_\eta^2 + h'\left(\psi_\eta\psi_{\xi\eta} - \psi_\xi\psi_{\eta\eta}\right) &= -p_\eta \\ -\varepsilon^2\left(\psi_{\xi\eta\eta} - h'\psi_{\eta\eta\eta}\right) - \varepsilon^4\left(\frac{\partial}{\partial\xi} - h'\frac{\partial}{\partial\eta}\right)^3\psi\end{aligned} \tag{2.11b}$$

The boundary conditions on the free surface $\eta = 0$ are obtained from (2.5a)-(2.5c) to read

$$\psi = 0 \tag{2.12a}$$

$$\varepsilon\left(h'p + \psi_{\eta\eta}\right) - \varepsilon^3\left[\left(\frac{\partial}{\partial\xi} - h'\frac{\partial}{\partial\eta}\right)^2\psi + 2h'\left(\psi_{\xi\eta} - h'\psi_{\eta\eta}\right)\right] = 0 \tag{2.12b}$$

$$p + \varepsilon^2\left(2\psi_{\xi\eta} - h'\psi_{\eta\eta}\right) - \varepsilon^4 h'\left(\frac{\partial}{\partial\xi} - h'\frac{\partial}{\partial\eta}\right)^2\psi = 0 \tag{2.12c}$$

The inner expansion for ψ begins with a term in ε^2. This is assumed, until there is evidence to the contrary. Thus, the expansion proceeds in powers of ε so that

$$\psi(\xi,\eta) = \varepsilon^2\Psi_2(\xi,\eta) + \varepsilon^3\Psi_3(\xi,\eta) + \cdots \tag{2.13}$$

Similarly, h is expanded as

$$h(\xi) = \varepsilon^{-1}\zeta(\xi) = h_0(\xi) + \varepsilon h_1(\xi) + \cdots \tag{2.14}$$

From (2.11)-(2.14), it is concluded that p is of order ε^4. Thus,

$$p(\xi,\eta) = \varepsilon^4 P_4(\xi,\eta) + \varepsilon^5 P_5(\xi,\eta) + \cdots \tag{2.15}$$

The velocity components are expanded as

$$u(\xi,\eta) = \varepsilon U_1(\xi,\eta) + \varepsilon^2 U_2(\xi,\eta) + \cdots \tag{2.16}$$

$$w(\xi,\eta) = \varepsilon^2 W_2(\xi,\eta) + \varepsilon^3 W_3(\xi,\eta) + \cdots \tag{2.17}$$

In this case, $U_1 = \Psi_{2\eta}$, $U_2 = \Psi_{3\eta}$ and $W_2 = -\Psi_{2\xi} + h'_0\Psi_{2\eta}$, etc.

2.3.1 Flow in the inner region to $O(\varepsilon^2)$

To leading order, the momentum equation, (2.11a) reads

$$\Psi_{2\eta}\Psi_{2\xi\eta} - \Psi_{2\xi}\Psi_{2\eta\eta} = \Psi_{2\eta\eta\eta} \tag{2.18}$$

The corresponding boundary conditions are obtained from (2.12a) and (2.12b), namely

$$\Psi_2(\xi,0) = \Psi_{2\eta\eta}(\xi,0) = 0 \tag{2.19}$$

To complete the problem for Ψ_2, another boundary condition is required. This is the matching condition, which will be obtained in chapter 3, namely

$$\Psi_2(\xi,\eta) \sim \frac{\eta^2}{2} \text{ as } \eta \to \infty \tag{2.20}$$

To leading order, the problem is similar to the case of the free jet (Tillett 1968) with different boundary conditions. A similarity solution can be carried out for Ψ_2; which is written here as

$$\Psi_2(\xi,\eta) = \xi^{2/3} f_2(\theta) \tag{2.21}$$

where $\theta = \eta\xi^{-1/3}$ is the similarity variable. The equation for $f_2(\theta)$ is given by

$$3f_2''' + 2f_2 f_2'' - f_2'^2 = 0 \tag{2.22}$$

subject to the following boundary conditions from (2.19) and (2.20):

$$f_2(0) = f_2''(0) = 0 \tag{2.23a}$$

$$f_2(\theta) \sim \frac{\theta^2}{2} \text{ as } \theta \to \infty \tag{2.23b}$$

An equation similar to (2.22) was investigated by Goldstein (1966) and revisited by Tillett (1968). For large θ, an asymptotic solution is possible to obtain, subject to condition (2.23b), namely

$$f_2(\theta \to \infty) = \frac{(\theta + c_1)^2}{2} + O\left[\exp\left(-\frac{2}{9}\theta^3\right)\right] \tag{2.24}$$

where c_1 is a constant determined from the numerical integration. The detail can be found in Appendix. Problem (2.22)-(2.23) is solved as an initial-value problem, where equation (2.22) is integrated subject to conditions (2.23a) and a guessed value of the slope at the origin. The problem was solved using Matlab's ODE45 subroutine which can be used to find the solution for an initial value problem. The slope (f_2') is adjusted in the program until reasonable matching up to 3rd decimal is achieved between the solution and the asymptotic form (2.23b) at large θ, or, more precisely, between f_2'' and 1. The integration is carried out over the domain $[0, \theta_\infty]$, where θ_∞ is a relatively large value of θ where matching is secured to within an imposed tolerance. The value of c_1 is then determined upon matching the numerical solution and its asymptotic counterpart (2.24). Figure 2.4 displays the dependence of f_2, f_2' and f_2'' on θ. In this figure the curve of f_2 represents the behaviour of the similarity function with respect to the similarity variable θ. Note that, to this order, $u = \varepsilon x^{1/3} f_2'$. Of particular interest is the slope at the origin $f_2'(0)$ which is directly related to the velocity at the free surface. From the figure it is seen that f_2' adjusts itself to behave linearly at shorter distance from origin, while the slope of f_2'' increases linearly very close to origin and then attains a constant value. For the purpose of the discussion here, it is convenient to observe that the initial slope is given approximately by $f_2'(0) \sim 1.6212$ and the value of c_1 is approximately equal to 0.9266. We can conclude from figure 2.4 that the velocity near the free surface increases linearly with height and further downstream the shear stress at the free surface attains a constant value.

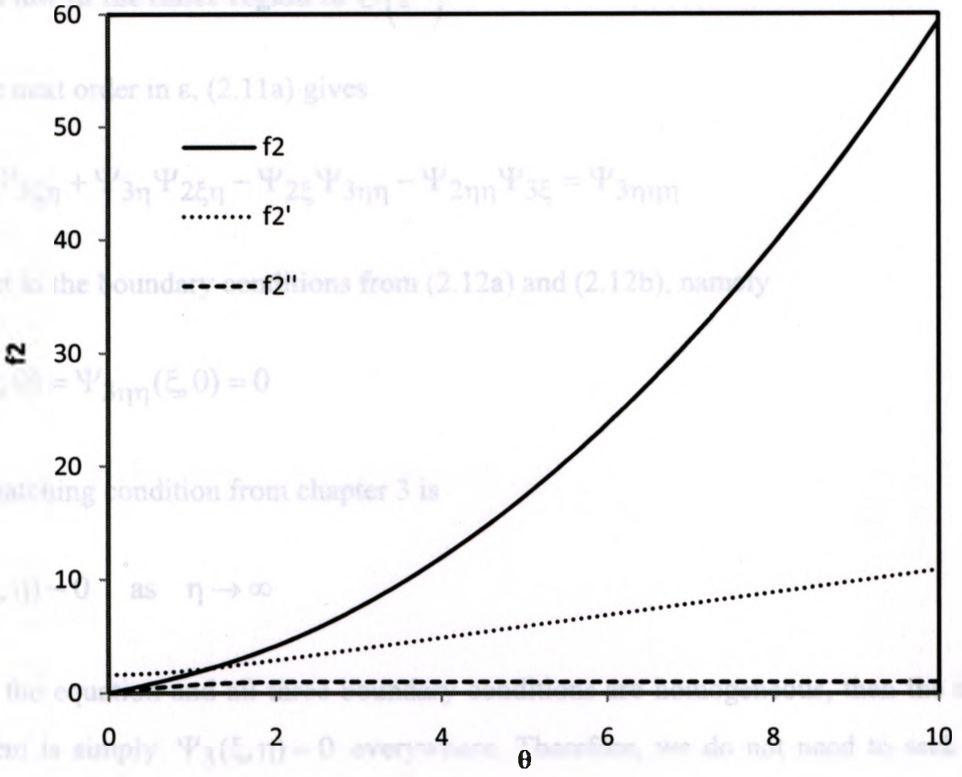

Figure 2.4: Variation of the similarity function f_2 with θ.

2.3.2 Flow in the inner region to $O(\varepsilon^3)$

To the next order in ε, (2.11a) gives

$$\Psi_{2\eta}\Psi_{3\xi\eta} + \Psi_{3\eta}\Psi_{2\xi\eta} - \Psi_{2\xi}\Psi_{3\eta\eta} - \Psi_{2\eta\eta}\Psi_{3\xi} = \Psi_{3\eta\eta\eta} \tag{2.25}$$

subject to the boundary conditions from (2.12a) and (2.12b), namely

$$\Psi_3(\xi,0) = \Psi_{3\eta\eta}(\xi,0) = 0 \tag{2.26a}$$

The matching condition from chapter 3 is

$$\Psi_3(\xi,\eta) \sim 0 \quad \text{as} \quad \eta \to \infty \tag{2.26b}$$

Since the equation and all three boundary conditions are homogeneous, then the solution to the problem is simply $\Psi_3(\xi,\eta) = 0$ everywhere. Therefore, we do not need to seek the similarity solution for Ψ_3 and proceed to the next order to acquire a better idea of the velocity profile.

2.3.3 The higher-order $O(\varepsilon^4)$ boundary layer

To the next order in ε i.e. $O(\varepsilon^4)$, the x momentum equation (2.11a) gives

$$\Psi_{4\eta\eta\eta} + \Psi_{2\xi}\Psi_{4\eta\eta} + \Psi_{2\eta\eta}\Psi_{4\xi} - \Psi_{2\eta}\Psi_{4\xi\eta} - \Psi_{2\xi\eta}\Psi_{4\eta} = G \tag{2.27}$$

where

$$G = P_{4\xi} - h_0' P_{4\eta} - \Psi_{2\xi\xi\eta} + h_0'' \Psi_{2\eta\eta} + 2h_0' \Psi_{2\xi\eta\eta} - h_0'^2 \Psi_{2\eta\eta\eta} \tag{2.28}$$

To find the corresponding expression for G we must first calculate the pressure; this is found from z momentum equation (2.8b) together with the dynamic boundary condition (2.12c). These give

$$P_{4\eta}(\xi,\eta) = -\frac{1}{9}\xi^{-1}\{4f_2 f_2' - t\left(f_2'^2 + 2f_2 f_2'' + 3f_2'''\right)\} = -\frac{2}{27}\xi^{-1}\frac{d}{d\theta}(4f_2^2 - 2tf_2 f_2' - 3tf_2'' + 3f_2')$$

where $t = \theta + c_1$. Integrating $P_{4\eta}$ with the boundary condition of

$$P_4(\xi, 0) = -\frac{2}{3}\xi^{-\frac{2}{3}} f_2'(0)$$

we find that,

$$P_4(\xi, \eta) = -\frac{2}{27}\xi^{-\frac{2}{3}}(4f_2{}^2 - 2tf_2f_2' - 3tf_2'' + 3f_2') - \frac{4}{9}\xi^{-\frac{2}{3}} f_2'(0)$$

Therefore, from equation (2.28), we can write,

$$G = \xi^{-\frac{5}{3}} g(\theta)$$

where

$$g = \frac{1}{27}t(4f_2f_2' - 2tf_2'^2) + \frac{4}{81}(4f_2{}^2 - 2tf_2f_2' - 3tf_2{}'' + 3f_2') - \frac{2}{9}(tf_2'' - f_2' + \frac{1}{2}t^2 f_2{}''') + \frac{8}{27}f_2'(0).$$

After evaluating G, in order to match R.H.S. & L.H.S of (2.27) we have to choose a similarity variable for $\Psi_4(\xi, \eta)$. A similarity solution can be carried out for $\Psi_4(\xi, \eta)$ in the form

$$\Psi_4(\xi, \eta) = \xi^{-\frac{2}{3}} f_4(\theta) \tag{2.29}$$

Where the equation for $f_4(\theta)$ is given by,

$$f_4''' + \frac{2}{3}f_2 f_4'' + \frac{2}{3}f_2' f_4' - \frac{2}{3}f_2'' f_4 = g \tag{2.30}$$

The boundary conditions at $\eta = 0$ are, from (2.12a) and (2.12b),

$$\Psi_4(\xi,0)=0 \qquad \text{and} \qquad \Psi_{4\eta\eta}=2h_0'\Psi_{2\xi\eta}-h_0''\Psi_{2\eta} \tag{2.31}$$

In terms of f_4, from (2.31) it can be written as,

$$f_4(0)=0, \qquad f_4''(0)=\frac{4}{9}c_1 f_2'(0) \tag{2.32}$$

The corresponding results for (2.30) are

$$g=\frac{8}{27}f_2'(0)+O(e^{-\frac{2}{9}t^3}) \tag{2.33}$$

giving asymptotically a particular integral

$$-\frac{4}{9}f_2'(0)+O(e^{-\frac{2}{9}t^3})$$

And complementary function

$$B_4 t+O(e^{-\frac{2}{9}t^3})$$

We have, in any case

$$f_4(\theta)\sim B_4 t-\frac{4}{9}f_2'(0)+O(t^{-2}) \tag{2.34}$$

Figure 2.5 shows the variation of similarity function f_4 with θ. The figure suggests that f_4 linearly increases with θ. f_4' increases when θ is small, but remains constant with the increase in θ and there is rapid decrease in f_4'' and later it achieves a constant trend while θ is increasing.

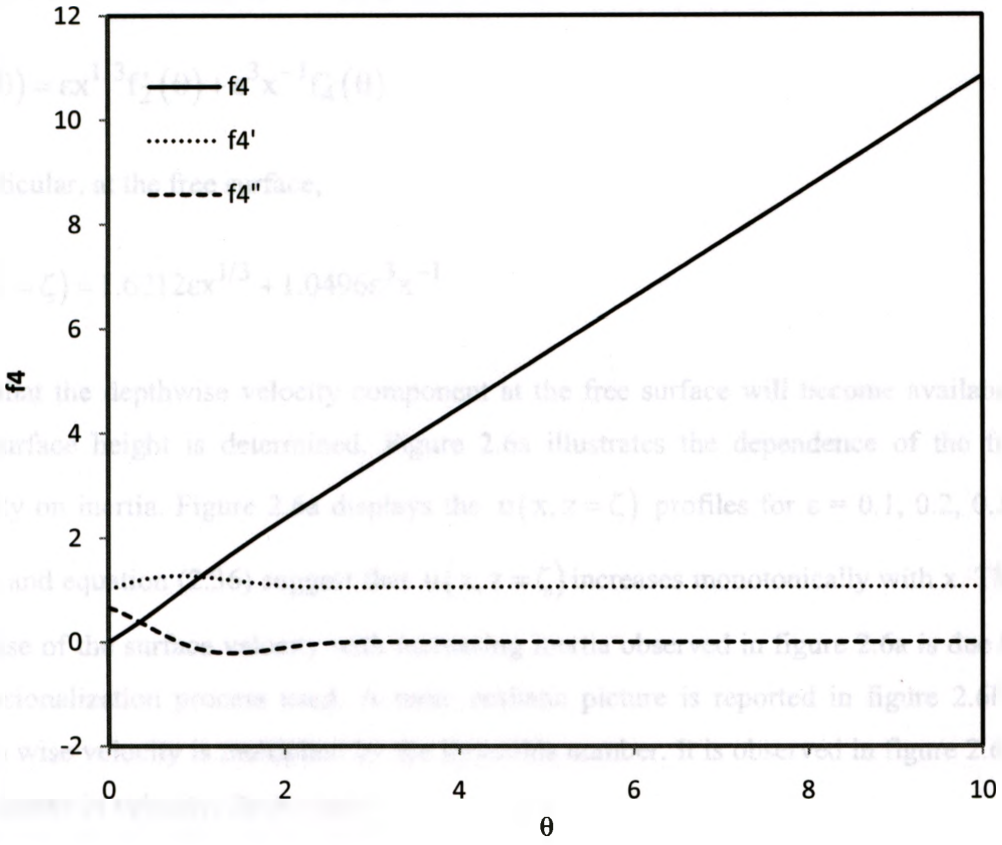

Figure 2.5: Variation of similarity function f_4 with θ

Therefore, from equation (2.16), the general expression of the velocity to fourth order becomes

$$u(x,\theta) = \varepsilon x^{1/3} f_2'(\theta) + \varepsilon^3 x^{-1} f_4'(\theta) \tag{2.35}$$

In particular, at the free surface,

$$u(x, z=\zeta) = 1.6212\varepsilon x^{1/3} + 1.0496\varepsilon^3 x^{-1} \tag{2.36}$$

Note that the depthwise velocity component at the free surface will become available once the free surface height is determined. Figure 2.6a illustrates the dependence of the free surface velocity on inertia. Figure 2.6a displays the $u(x, z=\zeta)$ profiles for ε = 0.1, 0.2, 0.3. Both the figure and equation (2.36) suggest that $u(x, z=\zeta)$ increases monotonically with x. The apparent decrease of the surface velocity with increasing inertia observed in figure 2.6a is due to the non-dimensionalization process used. A more realistic picture is reported in figure 2.6b. Here the stream wise velocity is multiplied by the Reynolds number. It is observed in figure 2.6b that with the increase in velocity, Re increases.

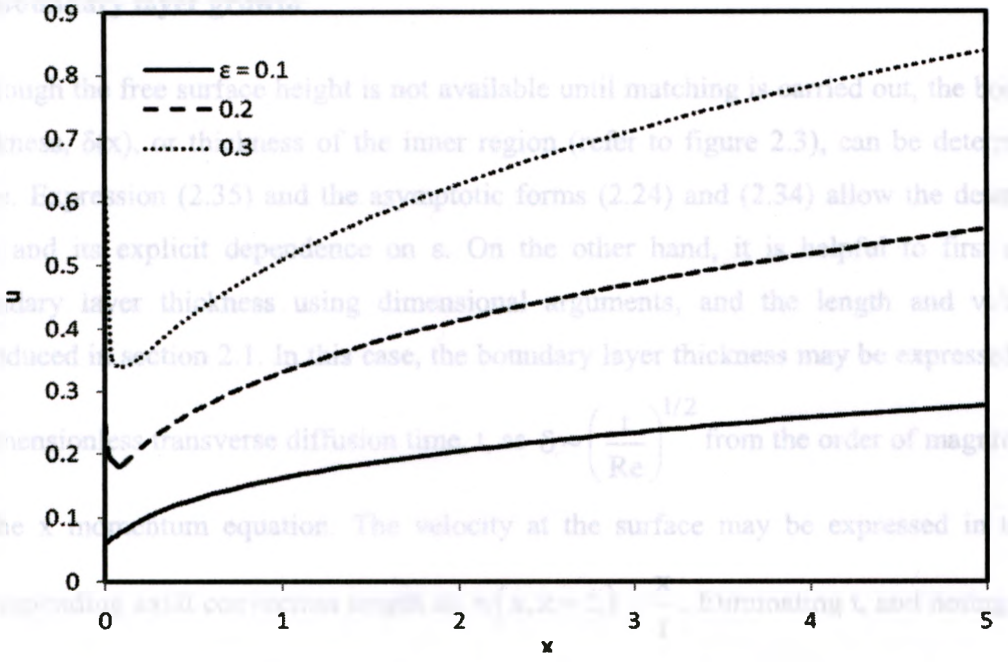

(a)

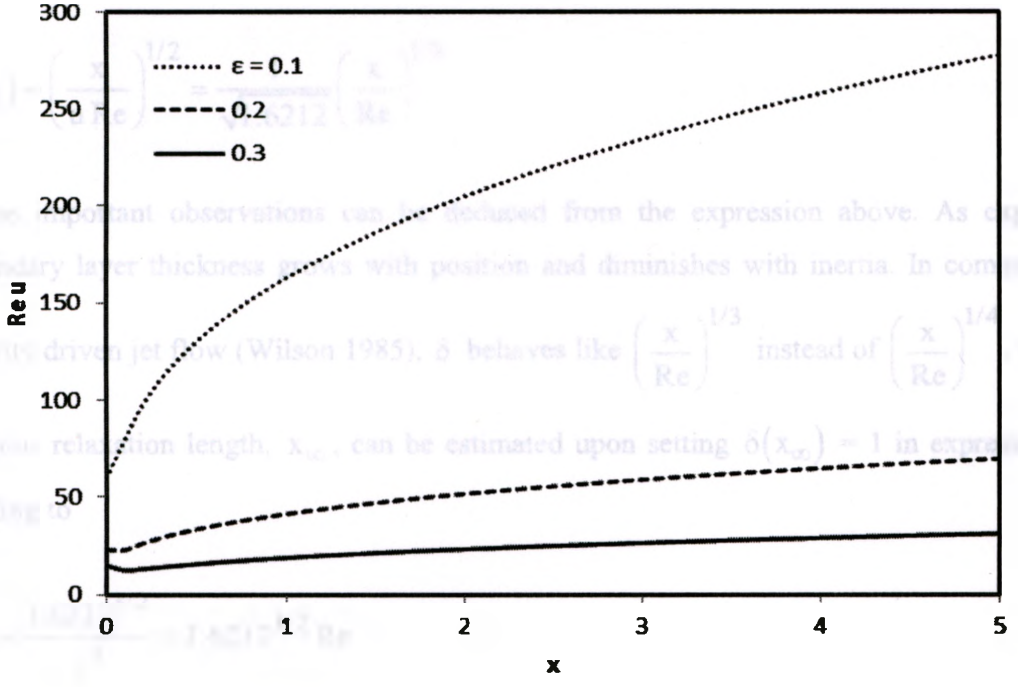

Figure 2.6: (a) Streamwise velocity u(x, z = ζ) versus x for different ε and (b) Scaled streamwise velocity u(x, z = ζ) versus x

2.4 Boundary layer growth

Although the free surface height is not available until matching is carried out, the boundary layer thickness, $\delta(x)$, or thickness of the inner region (refer to figure 2.3), can be determined at this stage. Expression (2.35) and the asymptotic forms (2.24) and (2.34) allow the determination of $\delta(x)$ and its explicit dependence on ε. On the other hand, it is helpful to first estimate the boundary layer thickness using dimensional arguments, and the length and velocity scales introduced in section 2.1. In this case, the boundary layer thickness may be expressed in terms of a dimensionless transverse diffusion time, t, as $\delta \sim \left(\frac{t}{Re}\right)^{1/2}$ from the order of magnitude analysis of the x momentum equation. The velocity at the surface may be expressed in terms of the corresponding axial convection length as $u(x, z=\zeta) \sim \frac{x}{t}$. Eliminating t, and noting from (2.36) that $u(x, z=\zeta) \sim 1.6212\varepsilon x^{1/3}$ to leading order, yield the following estimate:

$$\delta(x) \sim \left(\frac{x}{u\,Re}\right)^{1/2} = \frac{1}{\sqrt{1.6212}}\left(\frac{x}{Re}\right)^{1/3} \tag{2.37}$$

Some important observations can be deduced from the expression above. As expected, the boundary layer thickness grows with position and diminishes with inertia. In comparison with gravity driven jet flow (Wilson 1985), δ behaves like $\left(\frac{x}{Re}\right)^{1/3}$ instead of $\left(\frac{x}{Re}\right)^{1/4}$. In fact, the viscous relaxation length, x_∞, can be estimated upon setting $\delta(x_\infty) = 1$ in expression (2.37), leading to

$$x_\infty = \frac{1.6212^{3/2}}{\varepsilon^3} = 1.6212^{3/2}\,Re \tag{2.38}$$

Expressions (2.37) and (2.38) predict that the boundary layer thickness diminishes with increasing relaxation distance. The relaxation length is simply proportional to Re. Interestingly, both the actual (dimensional) viscous relaxation length and the shear stress at the lower wall increase linearly with C, and the relaxation length increases like D^2. For $x > x_\infty$, the boundary

layer contains the entire jet width and the nature of the flow depends on the fully developed flow in the channel.

For a more accurate estimate of δ, consider first the variation of the velocity profiles with respect to height, η, at different x position and ε, displayed in figure 2.7. The figure shows the gradual flattening of the velocity profile near the free surface as inertia decreases. The boundary layer height coincides with the level at which the asymptotic and inner velocity profiles begin to merge, as demonstrated in the figure. The influence of inertia on the boundary layer thickness is illustrated in figure 2.8, where the dependence of $\delta(x)$ on ε is shown. The boundary layer thickness typically grows with position x. Eventually, the inner region continues to grow with position as the film contracts, at which point the boundary layer prevails over the entire film width.

2.5 Conclusion

The inner region was analyzed in this chapter. The objective of the inner region was to find the solution of the equations of motion in the form of an "inner expansion" in ε. The higher order solution was pursued in the inner region in order to achieve the free surface velocity and boundary layer thickness.

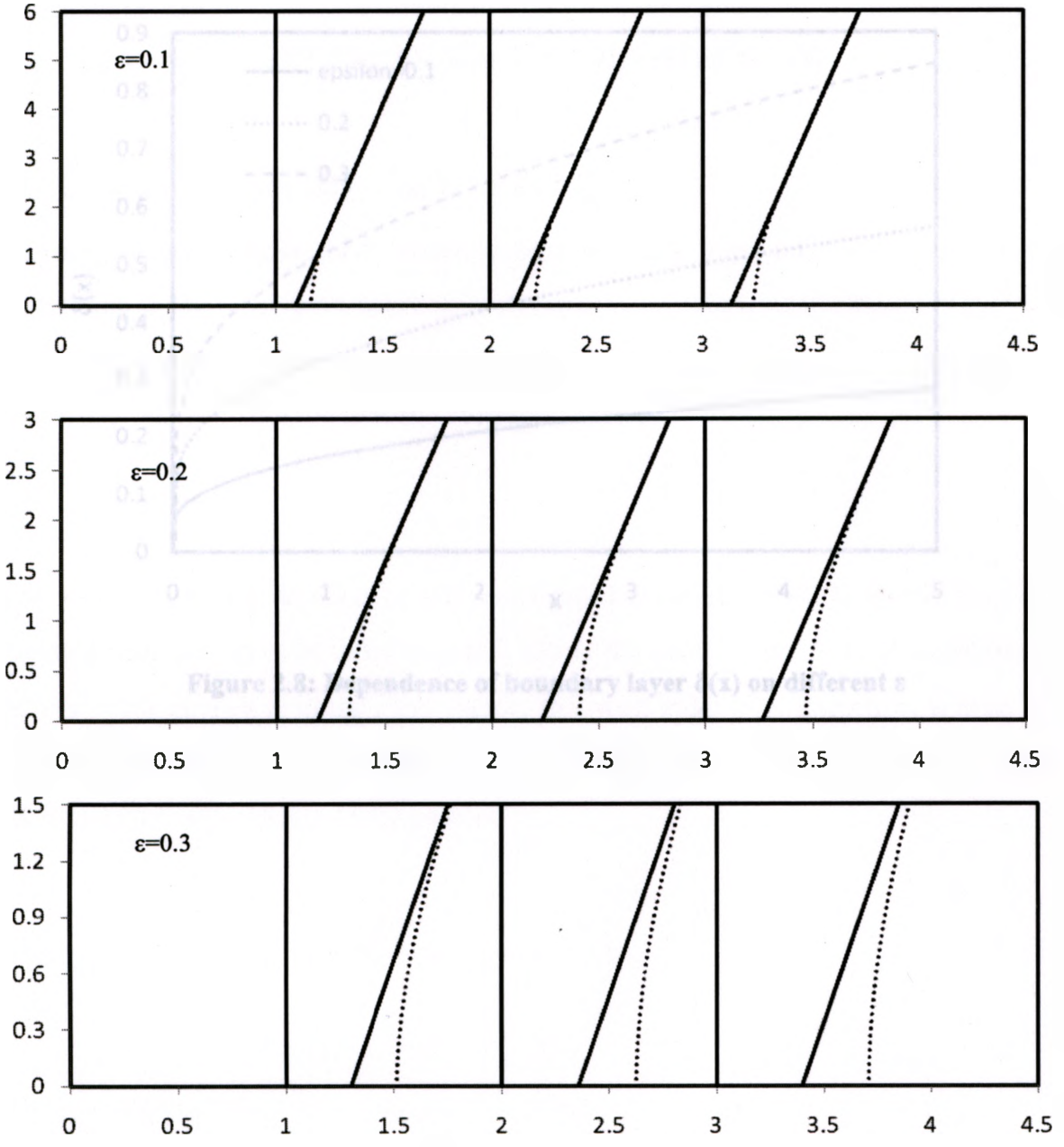

Figure 2.7: Dependence of streamwise velocity profiles for different ε on height, η, for different x position at epsilon=0.1, 0.2, 0.3 . Solid line indicates asymptotic behavior.

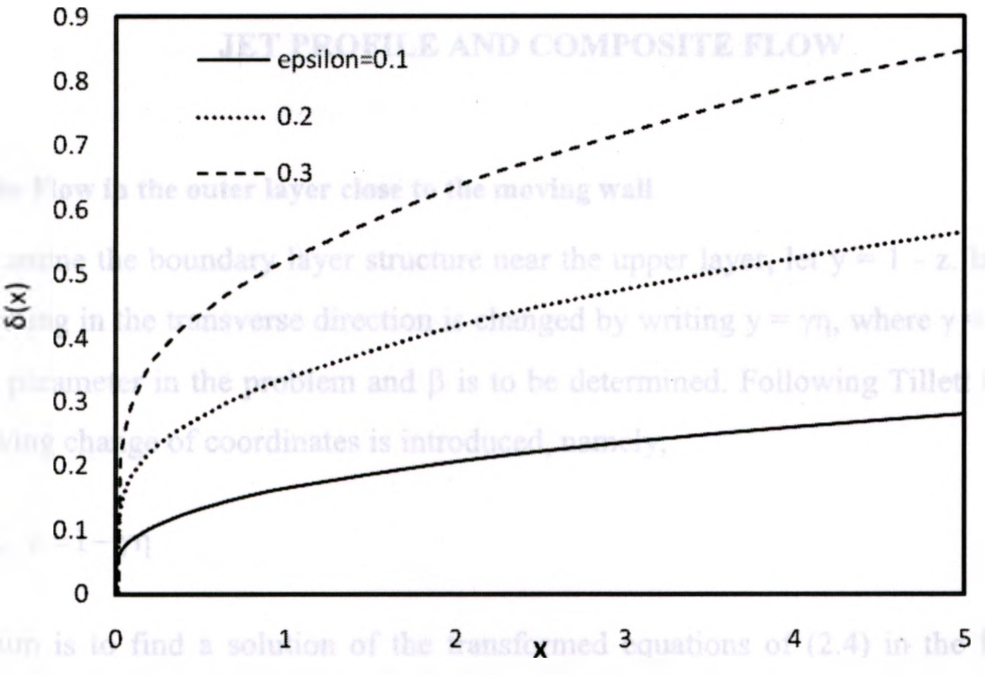

Figure 2.8: Dependence of boundary layer δ(x) on different ε

CHAPTER-3

JET PROFILE AND COMPOSITE FLOW

3.1 The Flow in the outer layer close to the moving wall

To examine the boundary layer structure near the upper layer, let y = 1 - z. In this case, the scaling in the transverse direction is changed by writing $y = \gamma\eta$, where $\gamma = Re^{-\beta}$ is the small parameter in the problem and β is to be determined. Following Tillett (1968), the following change of coordinates is introduced, namely,

$$x = \xi, \quad z = 1 - \gamma\eta \tag{3.1}$$

The aim is to find a solution of the transformed equations of (2.4) in the form of an "outer expansion" in γ. In order to match this to the core couette flow, it is necessary to have $\psi \sim 1/2$ as $\eta \to \infty$ in the outer region, to lowest order in γ. Therefore, ψ must be of order 1. Similarly to jet flow (Tillett 1968), the value of β is determined by requiring that the convective and viscous terms balance.

$$\psi_\eta\psi_{\xi\eta} - \psi_\xi\psi_{\eta\eta} = -\gamma^2 p_\xi - \gamma^{\left(\frac{1}{\beta}-1\right)}\psi_{\eta\eta\eta} - \gamma^{\left(\frac{1}{\beta}+1\right)}\psi_{\xi\xi\eta} \tag{3.2a}$$

$$\psi_\eta\psi_{\xi\xi} - \psi_\xi\psi_{\xi\eta} = p_\eta - \gamma^{\left(\frac{1}{\beta}-1\right)}\psi_{\xi\eta\eta} - \gamma^{\left(\frac{1}{\beta}+1\right)}\psi_{\xi\xi\xi} \tag{3.2b}$$

In this case, $\beta = 1$, and $\gamma = \varepsilon^3$. The components u, the streamwise velocity, and w, the transverse velocity, are now expressed in terms of the stream function as

$$u = \psi_z = -\frac{1}{\gamma}\psi_\eta \tag{3.3a}$$

$$w = -\psi_x = -\psi_\xi \tag{3.3b}$$

From (3.3a), it is obvious that u is of order $1/\gamma$. Considering the fact that u in the outer region must match the velocity in the core region: $u \to z$, it is also inferred that u must be of order $1/\gamma$ inside the outer region. The order of w can be found using the continuity equation when written in terms of inner variables, or

$$\gamma u_\xi - w_\eta = 0 \tag{3.4}$$

Thus, w is of order 1. The momentum conservation equations (3.2) are re-written as

$$\psi_\eta \psi_{\xi\eta} - \psi_\xi \psi_{\eta\eta} = -\gamma^2 p_\xi - \psi_{\eta\eta\eta} - \gamma^2 \psi_{\xi\xi\eta} \tag{3.5a}$$

$$\psi_\eta \psi_{\xi\xi} - \psi_\xi \psi_{\xi\eta} = p_\eta - \psi_{\xi\eta\eta} - \gamma^2 \psi_{\xi\xi\xi} \tag{3.5b}$$

The boundary conditions on the upper wall $\eta = 0$ are obtained from (2.6a) to read

$$\psi_\eta = -\gamma \text{ and } \psi_\xi = 0 \tag{3.6a}$$

$$\psi(\xi \to -\infty, \eta) = \frac{(1-\gamma\eta)^2}{2} \tag{3.6b}$$

The expansion proceeds in powers of γ so that

$$\psi(\xi,\eta) = \Psi_0(\xi,\eta) + \gamma\Psi_1(\xi,\eta) + \gamma^2\Psi_2(\xi,\eta) + \cdots \tag{3.7}$$

From (3.5), it is concluded that p is of order 1. Thus,

$$p(\xi,\eta) = P_0(\xi,\eta) + \gamma P_1(\xi,\eta) + \gamma^2 P_2(\xi,\eta) + \cdots \tag{3.8}$$

The velocity components are expanded as

$$u(\xi,\eta) = \gamma^{-1}U_{-1}(\xi,\eta) + U_0(\xi,\eta) + \gamma U_1(\xi,\eta) + \cdots \tag{3.9}$$

$$w(\xi,\eta) = W_0(\xi,\eta) + \gamma W_1(\xi,\eta) + \gamma^2 W_2(\xi,\eta) + \cdots \tag{3.10}$$

In this case, $U_{-1} = -\Psi_{0\eta}$, $U_0 = -\Psi_{1\eta}$, $U_1 = -\Psi_{2\eta}$, and $W_0 = -\Psi_{0\xi}$, etc.

To leading order, the equation for Ψ_0 and corresponding boundary conditions read

$$\Psi_{0\eta}\Psi_{0\xi\eta} - \Psi_{0\xi}\Psi_{0\eta\eta} = -\Psi_{0\eta\eta\eta} \tag{3.11a}$$

$$\Psi_{0\eta}\Psi_{0\xi\xi} - \Psi_{0\xi}\Psi_{0\xi\eta} = P_{0\eta} - \Psi_{0\xi\eta\eta} \tag{3.11b}$$

subject to

$$\Psi_{0\xi}(\xi,\eta=0) = \Psi_{0\eta}(\xi,\eta=0) = 0, \qquad \Psi_0(\xi,\eta\to\infty) = \frac{1}{2} \tag{3.12}$$

The solution to this problem is $\Psi_0(\xi,\eta) = \frac{1}{2}$, $P_{0\eta}(\xi,\eta) = 0$. Thus, $P_0(\xi,\eta)$ does not change with height, and will have to match the leading order term in the core region. In this case, since the pressure is of $O(\varepsilon^3)$ in the core region, then $P_0(\xi,\eta) = 0$

To order γ, the problem is governed by

$$\Psi_{0\eta}\Psi_{1\xi\eta} + \Psi_{1\eta}\Psi_{0\xi\eta} - \Psi_{1\xi}\Psi_{0\eta\eta} - \Psi_{0\xi}\Psi_{1\eta\eta} = -\Psi_{1\eta\eta\eta} \tag{3.13a}$$

$$\Psi_{1\eta}\Psi_{0\xi\xi} + \Psi_{0\eta}\Psi_{1\xi\xi} - \Psi_{1\xi}\Psi_{0\xi\eta} - \Psi_{0\xi}\Psi_{1\xi\eta} = P_{1\eta} - \Psi_{1\xi\eta\eta} \tag{3.13b}$$

$$\Psi_{1\eta\eta\eta}(\xi,\eta) = 0, \; P_{1\eta}(\xi,\eta) = \Psi_{1\xi\eta\eta} = 0$$

$$\Psi_{1\xi}(\xi,\eta=0) = 0, \Psi_{1\eta}(\xi,\eta=0) = -1, \Psi_1(\xi,\eta\to\infty) = -\eta$$

The solution of this problem is $\Psi_1(\xi,\eta) = -\eta$

To order γ^2, one has

$$\Psi_{2\xi}\Psi_{0\xi\eta}+\Psi_{1\eta}\Psi_{1\xi\eta}+\Psi_{0\eta}\Psi_{2\xi\eta}-\Psi_{2\xi}\Psi_{0\eta\eta}-\Psi_{1\xi}\Psi_{1\eta\eta}-\Psi_{0\xi}\Psi_{2\eta\eta} = -P_{0\xi}-\Psi_{0\xi\xi\eta}-\Psi_{2\eta\eta\eta} \tag{3.14a}$$

$$\Psi_{2\eta}\Psi_{0\xi\xi}+\Psi_{1\eta}\Psi_{1\xi\xi}+\Psi_{0\eta}\Psi_{2\xi\xi}-\Psi_{2\xi}\Psi_{0\xi\eta}-\Psi_{1\xi}\Psi_{1\xi\eta}-\Psi_{0\xi}\Psi_{2\xi\eta} = P_{2\eta}-\Psi_{2\xi\eta\eta}-\Psi_{0\xi\xi\xi} \tag{3.14b}$$

$$\Psi_{2\xi}(\xi,\eta=0)=0,\Psi_{2\eta}(\xi,\eta=0)=\eta, \qquad \Psi_2(\xi,\eta\to\infty)=\frac{1}{2}\eta^2$$

$$P_{0\xi}(\xi,\eta)=-\Psi_{2\eta\eta\eta}=0$$

$$P_{2\eta}(\xi,\eta)=\Psi_{2\xi\eta\eta}=0$$

The solution to this problem is $\Psi_2(\xi,\eta)=\frac{1}{2}\eta^2$

3.2The flow in the core regions (inside and outside the channel)

It is convenient to define the core region as comprising the core regions outside the channel ($x > 0$) and inside the channel upstream from the exit ($x < 0$). Ultimately, the flows inside and outside the channel must match at the channel exit ($x = 0$). However, this matching is only required between the two core regions. In contrast, given the boundary layer character of the inner regions (inside and outside the channel), similarity solutions can be sought separately. In other words, the presence of the singularity at the origin ($x = 0$, $z = 0$) prohibits any matching, but can be totally avoided in the current formulation. In this case, the inner solution inside the channel ($x < 0$) is not required for the determination of the flow outside the channel, and therefore will not be discussed any further.

In the core region, which is far from the region near $z = 0$, equations (2.4) must be solved, and are conveniently rewritten here as

$$\psi_z\psi_{xz}-\psi_x\psi_{zz}=-p_x+\varepsilon^3(\psi_{xxz}+\psi_{zzz}) \tag{3.15a}$$

$$-\psi_z\psi_{xx}+\psi_x\psi_{xz}=-p_z-\varepsilon^3(\psi_{xxx}+\psi_{xzz}) \tag{3.15b}$$

In this case, ψ and p are represented by the following expansions:

$$\psi(x,z) = \psi_0(x,z) + \varepsilon\psi_1(x,z) + \cdots \tag{3.16a}$$

$$p(x,z) = p_0(x,z) + \varepsilon p_1(x,z) + \cdots \tag{3.16b}$$

Here, recall that $\psi_0 = \frac{z^2}{2}$ is just the basic Couette flow stream function given in (2.3); ψ_m ($m > 0$) are higher order terms that denote the deviation from the basic flow due to its interaction with the boundary layer. Expansions (3.16) are similar to (2.1) for the flow with constriction (Smith 1979). Note, however, that, in contrast to (3.16a), Smith's leading order term in (2.1) does not exactly correspond to fully developed flow, but still satisfy the inviscid equations of motion. Quoting Tillett (1968), "Since the governing equations are elliptic (in x), this deviation will extend also to the region $x < 0$ in the channel." Based on these assumptions, upon inserting expressions (3.16) into equations (2.4), a hierarchy of equations is obtained to each order. To leading order $p_0(x, z) = 0$. For $m = 1$ and 2, the matching conditions obtained in section 3.3, and the condition $\psi_{m>0}(x \to -\infty, z) = 0$, lead to the vanishing of the stream function and pressure everywhere. More explicitly,

For $m = 1$, one has

$$\psi_{0z}\psi_{1xz} - \psi_{0zz}\psi_{1x} = -p_{1x} \tag{3.17a}$$

$$-\psi_{0z}\psi_{1xx} = -p_{1z} \tag{3.17b}$$

Upon eliminating p_1 from (3.17a) and (3.17b), the following equation is obtained for ψ_1:

$$\nabla^2\psi_{1x} - \frac{\psi_{0zzz}}{\psi_{0z}}\psi_{1x} = 0 \tag{3.18}$$

where $\nabla^2 = \frac{\partial^2}{\partial x^2} + \frac{\partial^2}{\partial z^2}$. Noting that $w_1 = -\psi_{1x}$, the following boundary-value problem in the ranges $-\infty \le x \le \infty$ and $0 \le z \le 1$ is concluded:

$$\nabla^2 w_1 = 0 \tag{3.19}$$

$$w_1(x,1) = 0,$$
$$w_1(x,0) = 0 \qquad \text{for} \quad x < 0,$$
$$w_1(x, z \to 0) = 0 = -\lambda_1(x) \qquad \text{for} \quad x > 0,$$
$$w_1 \quad \text{bounded as } |x| \to \infty.$$

The matching condition obtained in section 3.3 gives $\lambda_1(x) = 0$. In this case, the (unique) solution to the boundary-value problem (3.19) is $w_1(x, z) = 0$ for any x and z. Consequently, and since $\psi_1(x \to -\infty, z) = 0$, then $\psi_1(x, z)$ and $p_1(x, z)$ must vanish everywhere.

For m = 2, 3 following the similar procedure, w_2 and w_3 vanishes and consequently $\psi_2(x\ z)$, $\psi_3(x\ z)$, $p_2(x, z)$ and $p_3(x, z)$ also vanishes everywhere. More explicitly,

$$\psi_1(x, z) = \psi_2(x, z) = \psi_3(x, z) = p_1(x, z) = p_2(x, z) = p_3(x, z) = 0$$

3.3 Matching process

This section is introduced in order to find out the way how the flow behaves outside the channel. To do this, matching at the interface of the inner and core region is necessary. As there is another region near the upper wall outside the channel, matching is also required between the outer and the core region. However, it is found that the flow in the outer region behaves as the flow in the core region (Couette) and that is why it will not be discussed in this section. On the other hand by matching between inner and core, the free surface behavior is obtained.

The matching rule employed by Van Dyke (1964) is adopted here, namely

$$E_n H_m \psi = H_m E_n \psi \tag{3.20}$$

where m and n are integers. Here, E_n is the core-expansion operator, which truncates immediately after the term of order ε^n where the expansion is expressed in terms of core variables. H_m is the corresponding inner-expansion operator. For successful application of the matching rule (3.20), the stretching transformation between the inner and core variables must be in the canonical form $y = \varepsilon\eta$. In this case, the core expansion must be written in terms of y, not z; otherwise (3.20) can be satisfied only approximately. It is required that the two expressions in (3.20) be exactly the same, for all m and n. Recall that, to leading order, the stream function in the core region is $\psi_0 = \frac{z^2}{2}$, which can be expressed using expansion of ψ (3.16), in the core region in terms of y and h, leading to

$$\psi = \frac{(y+\varepsilon h)^2}{2} + O(\varepsilon) \tag{3.21}$$

Consider first m = 2 and n = 0. Applying E_0 on (3.21) gives

$$E_0\psi = \frac{y^2}{2} \tag{3.22}$$

As this expression must be in inner variables when the operator H_2 is applied, $E_0\psi$ is rewritten in the form:

$$E_0\psi = \frac{\varepsilon^2\eta^2}{2} \tag{3.23}$$

Therefore,

$$H_2E_0\psi = \frac{\varepsilon^2\eta^2}{2} = \frac{y^2}{2} \tag{3.24}$$

To leading order, the inner expansion for the stream function is obtained from (2.13) as

$\psi = \varepsilon^2\Psi_2$. Thus $H_2\psi = \varepsilon^2\Psi_2$ and therefore,

$$E_0 H_2 \psi = E_0\left(\varepsilon^2 \Psi_2\right) \tag{3.25}$$

This leads to $\Psi_2 \sim \frac{\eta^2}{2}$ for large η. Large η means far from the inner region to the core region. This is the condition in (2.20) or equivalently (2.23b). Recall that this condition led to the determination of f_2. Consequently, from (2.13), (2.21) and (2.24), at large θ

$$H_2\psi = \varepsilon^2\Psi_2 = \varepsilon^2\xi^{2/3} f_2 = \varepsilon^2\xi^{2/3}\frac{(\theta + c_1)^2}{2} = \varepsilon^2\xi^{2/3}\frac{\left(\eta\xi^{-1/3} + c_1\right)^2}{2} \tag{3.26}$$

When (3.26) is expressed in terms of core variables, it becomes:

$$H_2\psi = \left[\frac{y^2}{2} + y\varepsilon c_1 x^{1/3} + \frac{\varepsilon^2}{2}\left(c_1 x^{1/3}\right)^2\right] \tag{3.27}$$

leading to

$$E_0 H_2 \psi = \frac{y^2}{2} \tag{3.28}$$

as required. So it can be seen that for n = 0 and m = 2, the inner and core expansions match, and (3.20) is satisfied. Similarly, taking n = 0 and m = 3, leads to

$$H_3 E_0 \psi = \frac{\varepsilon^2 \eta^2}{2} \tag{3.29}$$

$$E_0 H_3 \psi = E_0\left(\varepsilon^2 \Psi_2 + \varepsilon^3 \Psi_3\right)$$

which, upon matching with $E_0 H_3 \psi$, leads to $\Psi_3 \sim 0$, and consequently to condition (2.26b).

Next, (3.20) is considered with m = 2 and n = 1.

$$E_1\psi = \frac{y^2}{2} + y\varepsilon h_0 + \varepsilon\psi_1(x, y+\varepsilon h_0) \tag{3.30}$$

Expanding about y,

$$\psi_1(x, y+\varepsilon h_0) = \psi_1(x,y) + \varepsilon h_0\psi_{1y}(x,y) + \frac{(\varepsilon h_0)^2}{2}\psi_{1yy}(x,y)$$

Expanding the terms on the right-hand side about y = 0,

$$\psi_1(x, y+\varepsilon h_0) = \psi_1(x,0) + y\psi_{1y}(x,0) + \frac{y^2}{2}\psi_{1yy}(x,0) + \varepsilon h_0\psi_{1y}(x,0) + \varepsilon h_0 y\psi_{1yy}(x,0)$$
$$+ \frac{(\varepsilon h_0)^2}{2}\psi_{1yy}(x,0)$$

In this case, (3.30) reduces to

$$E_1\psi = \frac{y^2}{2} + y\varepsilon h_0 + \varepsilon\psi_1(x,0) + \varepsilon y\psi_{1y}(x,0) + \varepsilon\frac{y^2}{2}\psi_{1yy}(x,0) \tag{3.30a}$$

In terms of inner variable, $y = \varepsilon\eta$,

$$E_1\psi = \frac{\varepsilon^2\eta^2}{2} + \varepsilon^2\eta h_0 + \varepsilon\psi_1(x,0) + \varepsilon^2\eta\psi_{1y}(x,0) + \frac{\varepsilon^3\eta^2}{2}\psi_{1yy}(x,0) \tag{3.31}$$

In this case, noting that $y = \varepsilon\eta$ is small, one has

$$H_2E_1\psi = \frac{y^2}{2} + y\varepsilon h_0 + \varepsilon\psi_1(x,0) + \varepsilon y\psi_{1y}(x,0) \tag{3.32}$$

On the other hand, applying E_1H_2 on the inner expansion (2.13) and using (3.26) gives

$$E_1H_2\psi = \frac{y^2}{2} + \varepsilon c_1 x^{1/3} y \tag{3.33}$$

Comparing (3.32) and (3.33) leads to $\psi_1(x, 0) = 0$. As $w_n = - \psi_{nx}$, this leads in turn to the homogeneous boundary condition $\lambda_1(x) = -\psi_{1x}(x,0) = 0$ for the governing equation of w_1 (3.18). Since the unique solution of (3.18) is $w_1(x, z) = 0$ everywhere it can be concluded that $\psi_1(x, y) = 0$ everywhere is a solution for this problem (3.18). From this, one concludes that, $\psi_{1y}(x,0) = 0$, which also satisfies matching. The remaining terms in (3.32) and (3.33) then yield the result $h_0(x) = c_1 x^{1/3}$. In this case, the free surface height is given by

$$\zeta(x) = c_1 x^{1/3}\varepsilon + O\left(\varepsilon^2\right) \tag{3.34}$$

The vanishing of $\psi_1(x, z)$ means that, to the order ε, there is no interaction between the boundary layer and the core flow. In other words, as $\psi_1(x, z) = 0$ everywhere, there is no outcome from the matching at the interface between the inner and the core region The form of $h_0(x)$ obtained also ensures that (3.20) is satisfied for $m = 3$ and $n = 1$. The next step is to determine $\psi_2(x, z)$ and $h_1(x)$ by considering an analogous matching process to the above, using $m = n = 2$.

$$E_2\psi = \frac{y^2}{2} + y\varepsilon h_0 + y\varepsilon^2 h_1 + \frac{\varepsilon^2 {h_0}^2}{2} + \varepsilon^2\psi_2(x,0) + \varepsilon^2 y\psi_{2y}(x,0) \tag{3.35}$$

In terms of inner variable, $y = \varepsilon\eta$,

$$E_2\psi = \frac{\varepsilon^2\eta^2}{2} + \varepsilon^2\eta h_0 + \varepsilon^3\eta h_1 + \frac{\varepsilon^2 {h_0}^2}{2} + \varepsilon^2\psi_2(x,0) + \varepsilon^3\eta\psi_{2y}(x,0)$$

So,

$$H_2E_2\psi = \frac{y^2}{2} + y\varepsilon h_0 + \frac{\varepsilon^2 {h_0}^2}{2} + \varepsilon^2\psi_2(x,0)$$

and

$$E_2H_2\psi = \frac{y^2}{2} + c_1\varepsilon y x^{1/3} + \frac{\varepsilon^2}{2}c_1^2 x^{2/3} \tag{3.36}$$

This yields the fact that $\psi_2(x, 0) = 0$ in the core expansion, concluding that $\psi_2(x, z) = 0$ everywhere, reflecting the absence of interaction between the boundary layer and the core flow also to order ε^2.The next step is to determine $h_1(x)$ and $\psi_3(x, 0)$. For n = m = 3, one obtains

$$H_3E_3\psi = \frac{y^2}{2} + \varepsilon y h_0 + \varepsilon^2\left[y h_1 + \frac{h_0^2}{2}\right] + \varepsilon^3 h_0 h_1 + \varepsilon^3\psi_3(x,0) \tag{3.37}$$

$$E_3H_3\psi = E_3\left(\varepsilon^2\Psi_2\right) = \frac{y^2}{2} + y\varepsilon c_1 x^{1/3} + \frac{\varepsilon^2}{2}\left(c_1 x^{1/3}\right)^2 \tag{3.38}$$

Upon matching, the height of the free surface to the next order is determined, namely

$$h_1(x) = 0 \tag{3.39}$$

Also, the boundary condition, which is required to solve the boundary value problem in the core region, is obtained. Thus,

$$\psi_3(x,0) = 0 \tag{3.40}$$

For m=n=4

$$H_4E_4\psi = \frac{y^2}{2} + \varepsilon y h_0 + \varepsilon^2\left[y h_1 + \frac{h_0^2}{2}\right] + \varepsilon^3 h_0 h_1 + \varepsilon^3 y h_2 + \varepsilon^4\left[\frac{h_1^2}{2} + h_0 h_2 + \psi_4(x,0)\right]$$

$$= H_3E_3\psi + \varepsilon^3 y h_2 + \varepsilon^4\left[\frac{h_1^2}{2} + h_0 h_2 + \psi_4(x,0)\right]$$

$$E_4H_4\psi = \frac{y^2}{2} + y\varepsilon c_1 x^{1/3} + \frac{\varepsilon^2}{2}c_1^2 x^{2/3} + y\varepsilon^3 B_4 x^{-1} + \varepsilon^4 B_4 c_1 x^{-2/3}$$

$$= E_3H_3\psi + y\varepsilon^3 B_4 x^{-1} + \varepsilon^4 B_4 c_1 x^{-2/3}$$

Comparing $H_4E_4\psi$ and $E_4H_4\psi$, it is found that, $h_2 = B_4x^{-1}$ and $\psi_4(x, z=0)=0$

Even though $w_4(x, z)$ is not evaluated, it can be conjectured from the homogeneous solution of w_1, w_2 and w_3, that $w_4(x, z)$ will be zero everywhere leading to $\psi_4(x, z) = 0$ everywhere. However, the important result reached here from the matching process is the height of the free surface which is

$$\zeta(x)=\varepsilon c_1 x^{1/3}+\varepsilon^3 B_4 x^{-1} \tag{3.41}$$

3.4 Jet profiles

Figure 3.1 displays the dependence of free surface height on inertia. The surface profiles suggest a significant thickening of the film when inertia increases. The singularity is present in the free surface at the channel exit because of x^{-1} term. For the surface to exhibit minimum or maximum, $\frac{d\zeta(x)}{dx}=0$, resulting in $x_m=\left(\frac{3B_4\varepsilon^2}{c_1}\right)^{3/4}$. In this case, recall $c_1 = 0.9266$, and $B_4 = 1.0496$. The surface exhibits a maximum at a location given by $x_m=\left[3.399\varepsilon^2\right]^{3/4}$.

Figure 3.2 depicts the variation of surface curvature with inclination, ϕ, for $\varepsilon = 0.1, 0.2, 0.3$. It shows that the curvature increases with ϕ, reaching a maximum at some inclination, and decreases rapidly as $\phi \to 0^o$.

Figure 3.3 displays the asymptotic and numerical streamwise velocity profiles based on the inner layer solution (2.35), along with the free surface height. Note that the difference between figure 3.3 and figure 2.7 is that, the free surface height was not yet obtained in figure 2.7, and this latter was drawn in the (η, x) plane.

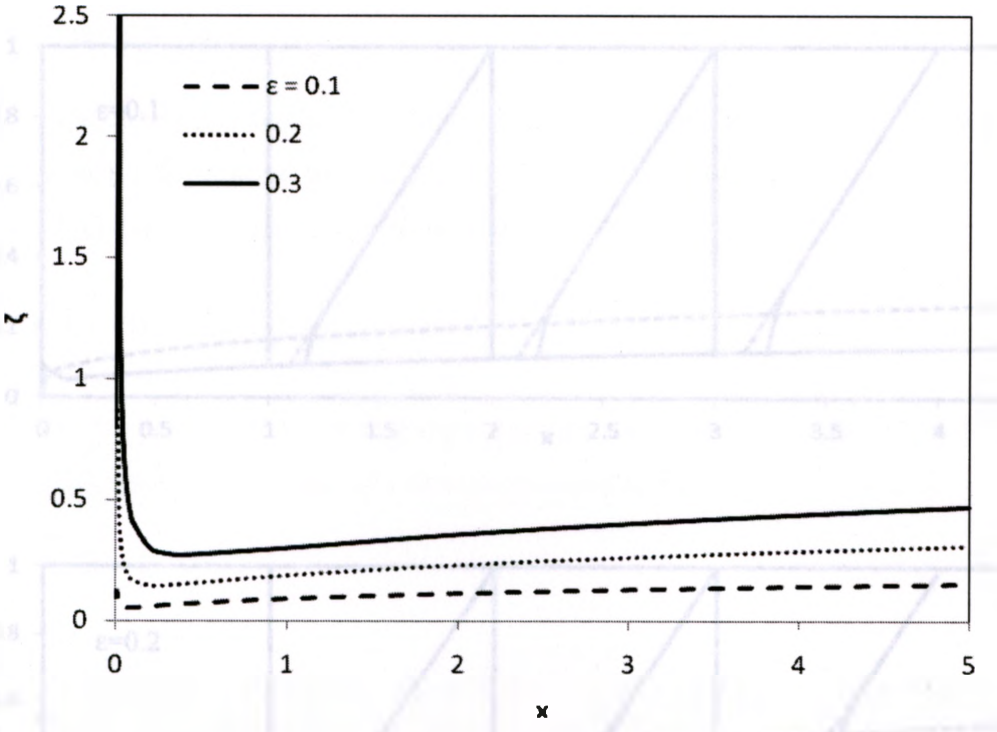

Figure 3.1: Variation of free surface height ζ(x) with position x at different ε

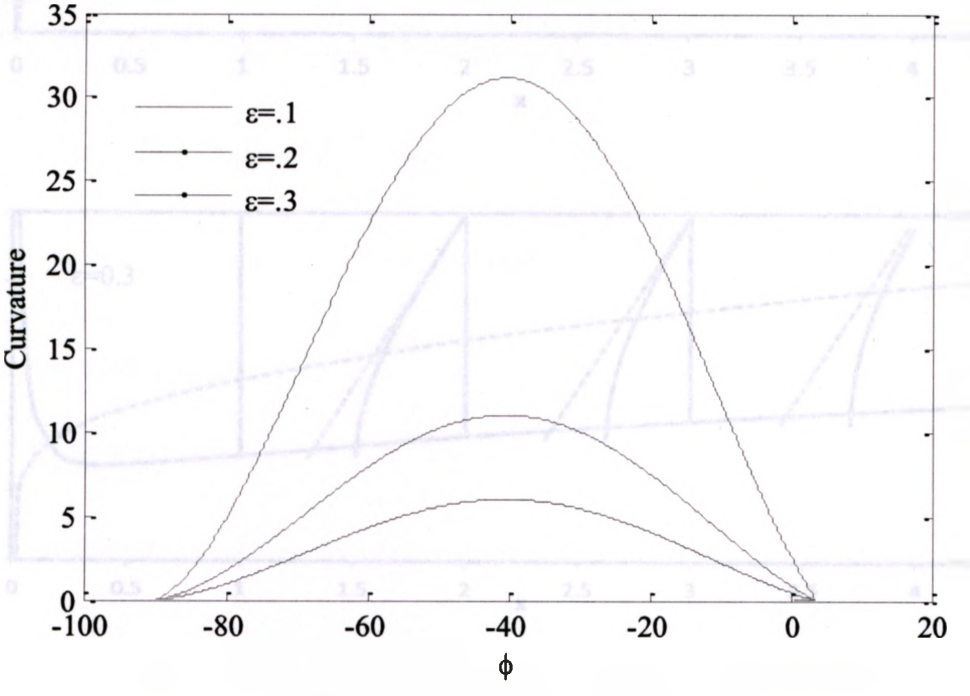

Figure 3.2: Curvature versus Φ

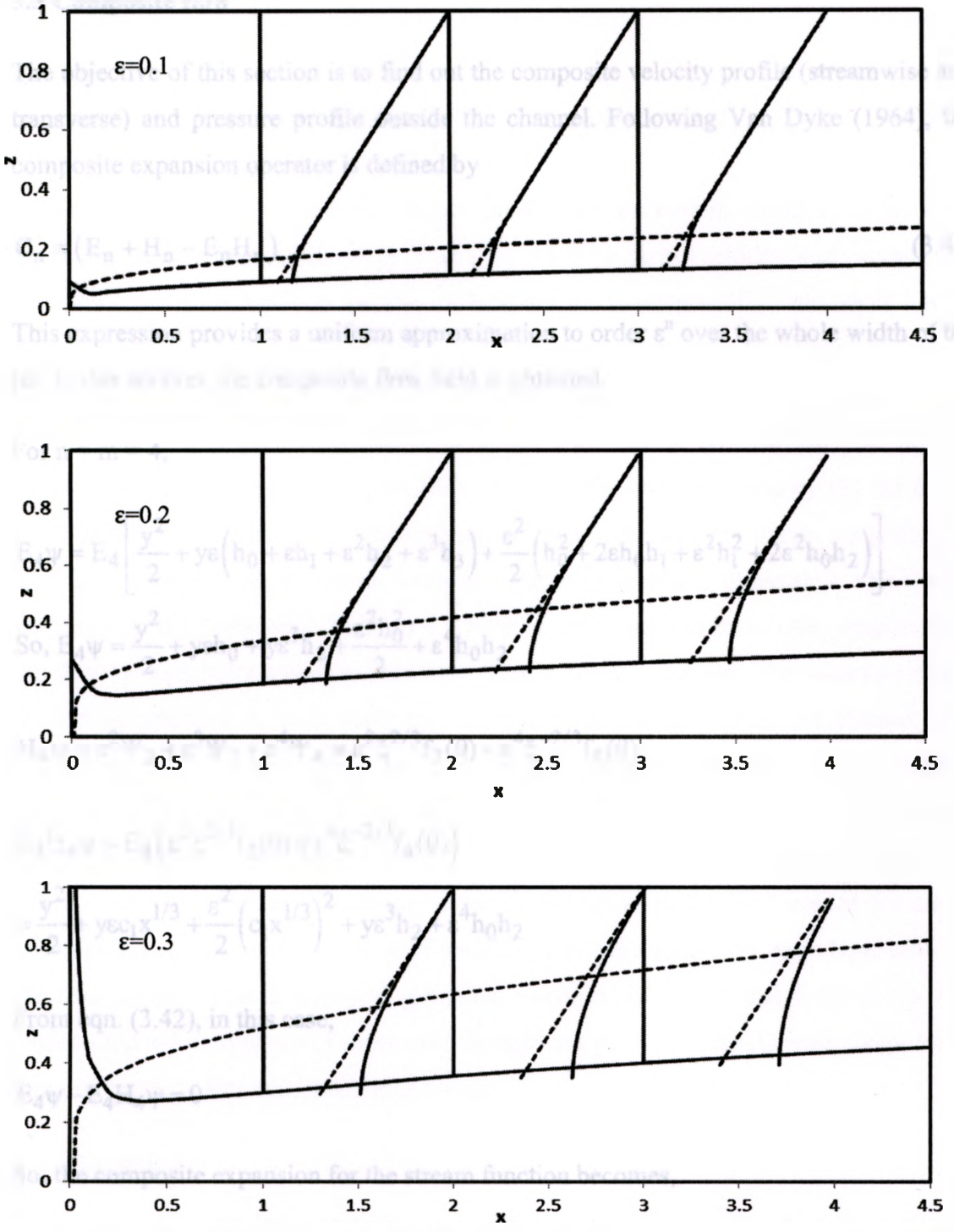

Figure 3.3: Variation of stream wise velocity profiles with z position for different x at ε = 0.1, 0.2, and 0.3. Dashed lines indicate asymptotic behavior.

3.5 Composite flow

The objective of this section is to find out the composite velocity profile (streamwise and transverse) and pressure profile outside the channel. Following Van Dyke (1964), the composite expansion operator is defined by

$$C_n \equiv (E_n + H_n - E_n H_n) \tag{3.42}$$

This expression provides a uniform approximation to order ε^n over the whole width of the jet. In this section, the composite flow field is obtained.

For $n = m = 4$,

$$E_4\psi = E_4\left[\frac{y^2}{2} + y\varepsilon\left(h_0 + \varepsilon h_1 + \varepsilon^2 h_2 + \varepsilon^3 h_3\right) + \frac{\varepsilon^2}{2}\left(h_0^2 + 2\varepsilon h_0 h_1 + \varepsilon^2 h_1^2 + 2\varepsilon^2 h_0 h_2\right)\right]$$

$$\text{So, } E_4\psi = \frac{y^2}{2} + y\varepsilon h_0 + y\varepsilon^3 h_2 + \frac{\varepsilon^2 h_0^2}{2} + \varepsilon^4 h_0 h_2$$

$$H_4\psi = \varepsilon^2\Psi_2 + \varepsilon^3\Psi_3 + \varepsilon^4\Psi_4 = \varepsilon^2\xi^{2/3} f_2(\theta) + \varepsilon^4\xi^{-2/3} f_4(\theta)$$

$$E_4 H_4\psi = E_4\left(\varepsilon^2\xi^{2/3} f_2(\theta) + \varepsilon^4\xi^{-2/3} f_4(\theta)\right)$$

$$= \frac{y^2}{2} + y\varepsilon c_1 x^{1/3} + \frac{\varepsilon^2}{2}\left(c_1 x^{1/3}\right)^2 + y\varepsilon^3 h_2 + \varepsilon^4 h_0 h_2$$

From eqn. (3.42), in this case,

$$E_4\psi - E_4 H_4\psi = 0$$

So, the composite expansion for the stream function becomes,

$$C_4\psi = H_4\psi + E_4\psi - E_4 H_4\psi = \varepsilon^2\xi^{2/3} f_2(\theta) + \varepsilon^4\xi^{-2/3} f_4(\theta) \tag{3.43}$$

The following expressions for the streamwise and transverse velocity components:

$$C_4 u = \varepsilon \xi^{1/3} f_2' + \varepsilon^3 \xi^{-1} f_4' \tag{3.44}$$

$$C_4 w = -\frac{\varepsilon^2}{3} \xi^{-1/3} \left[2f_2 - (\theta + c_1) f_2' \right] + \frac{\varepsilon^4}{3} \xi^{-5/3} \left[2f_4 + (\theta + c_1) f_4' - 3B_4 f_2' \right] \tag{3.45}$$

These expressions dictate how the velocity profile changes over the width of the jet up to the fourth order. The influence of inertia on the flow field (velocity and pressure) at different x positions between the free surface and the moving wall are shown in figures 3.4, 3.5 and 3.6. The u profiles in figures 3.4-3.6a indicate that the flow behaves close to fully developed at the channel exit, exhibiting a singularity like x^{-1} and further downstream, the u profile flattens at a location x. Further downstream, the flow is entrained by moving wall. In figure 2.6(a) the u profile shows singularity but the figure 3.4-3.6a this singularity is not visible because the profile was not drawn very close to exit. The w profiles show that the transverse velocity gradually diminishes with x after the jump at the channel exit. Figure 3.4-3.6b also shows that the transverse component of the flow is essentially absent except very close to the free surface. The velocity reflects the strong presence of both shear and elongation in the flow. Near the channel exit, elongation is clearly dominant at the free surface where most of the dissipation rate is concentrated. Further downstream, most of the dissipation occurs above the free surface. The pressure profiles in figure 3.4-3.6c suggest that the pressure changes rapidly near channel exit and further downstream pressure becomes essentially constant for any z position. There is a small departure of pressure from zero across the inner layer close to the free surface. This is expected given the vanishing of the normal force at the free surface and the dominance of shear over elongation rate. For a moving wall, the pressure remains finite, in fact maximum, at the wall.

3.6 Conclusion

The analysis of outer and core regions were performed in this chapter. Also the matching rule of Van Dyke (1964) was employed to obtain the boundary condition for the inner region and the shape of the unknown free surface. Again, composite matching was applied to find out the composite velocity profile (streamwise and transverse) and the pressure profile outside the channel.

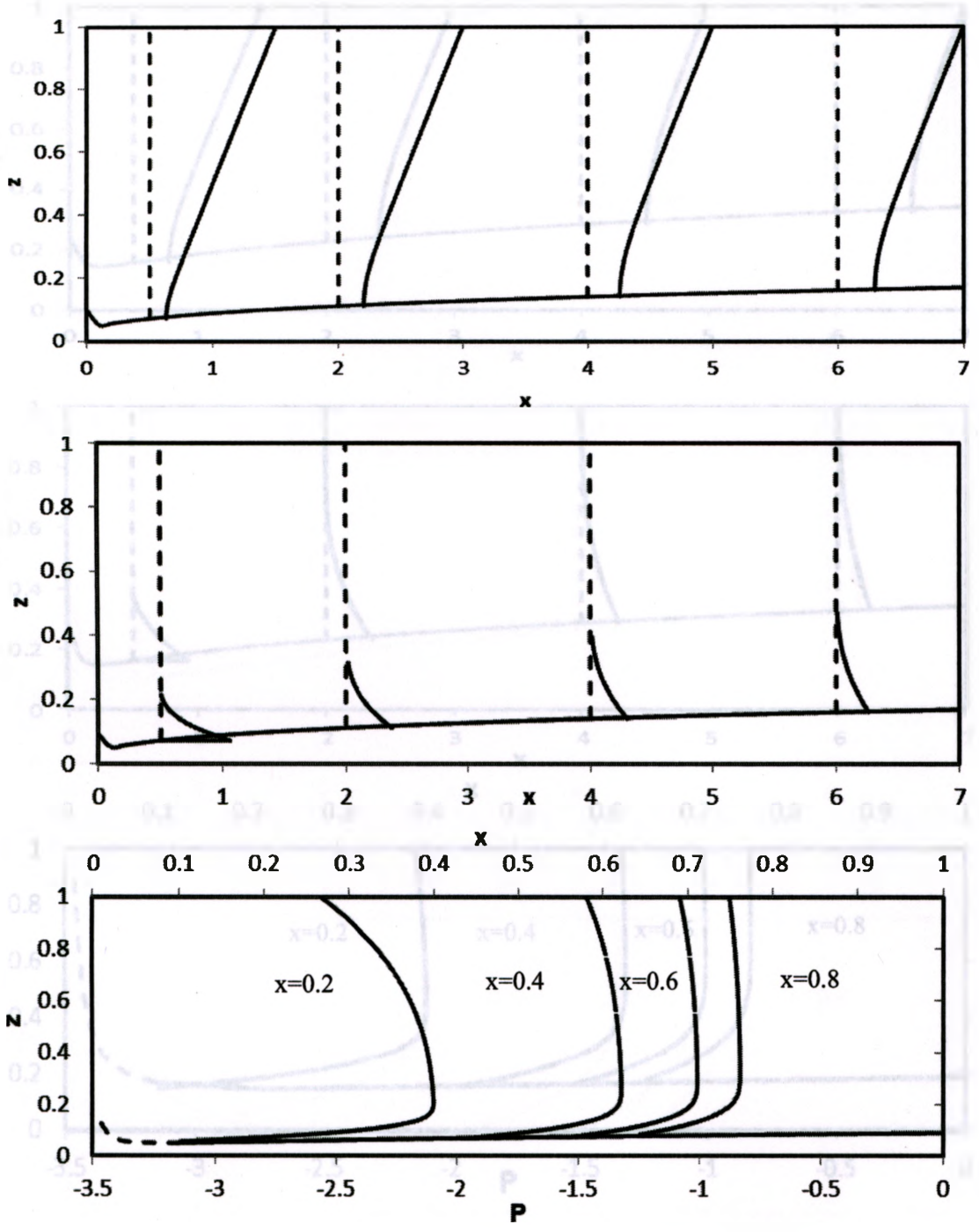

Figure 3.4: Variation of (a) streamwise velocity, (b) transverse velocity and (c) pressure profiles with position for ε = 0.1. Note: streamwise velocity and transverse velocity are drawn on same scale. The vertical dashed line is the origin at each position.

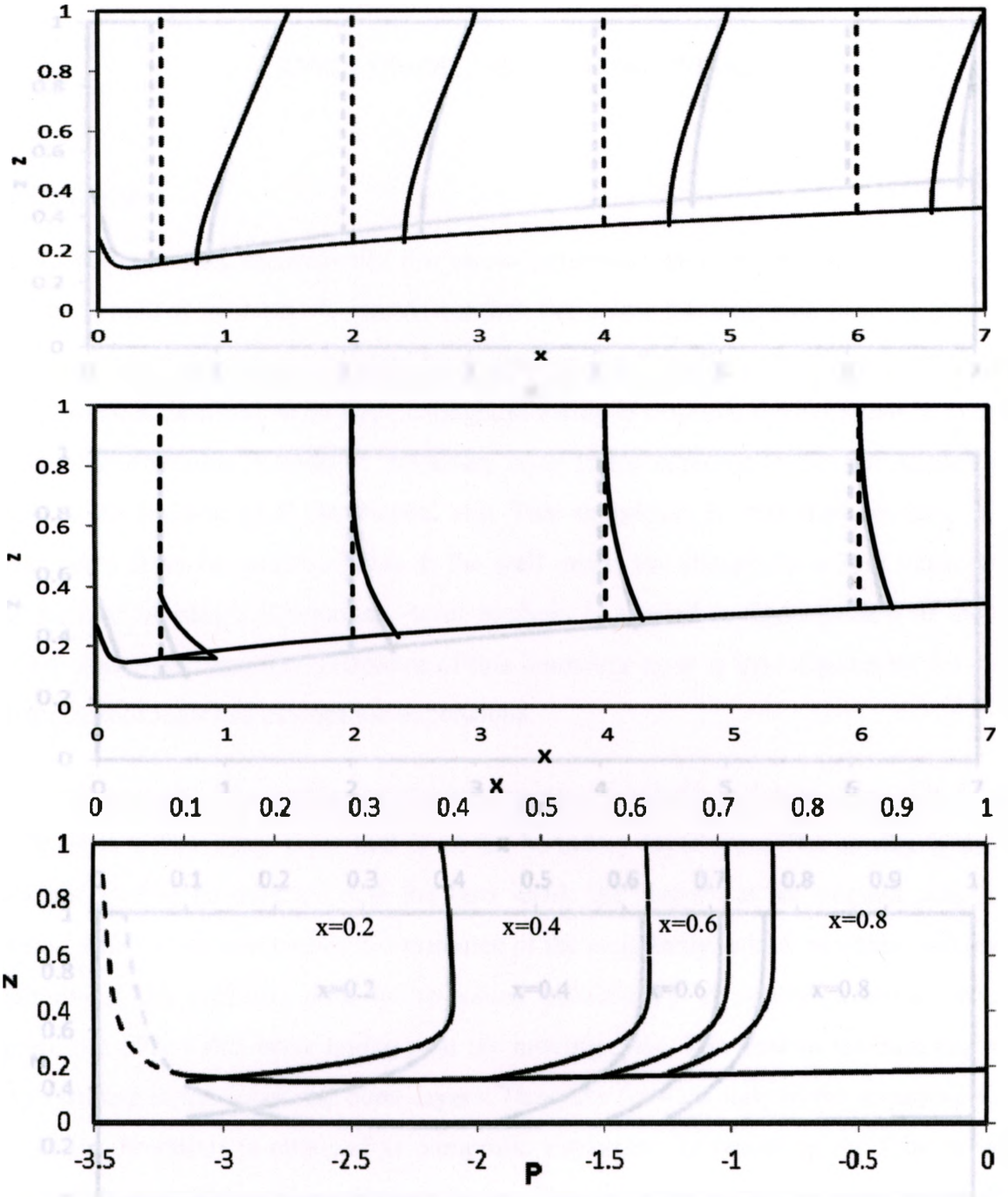

Figure 3.5: Variation of (a) streamwise velocity, (b) transverse velocity and (c) pressure profiles with position for ε = 0.2. Note: streamwise velocity and transverse velocity are drawn on same scale. The vertical dashed line is the origin at each position.

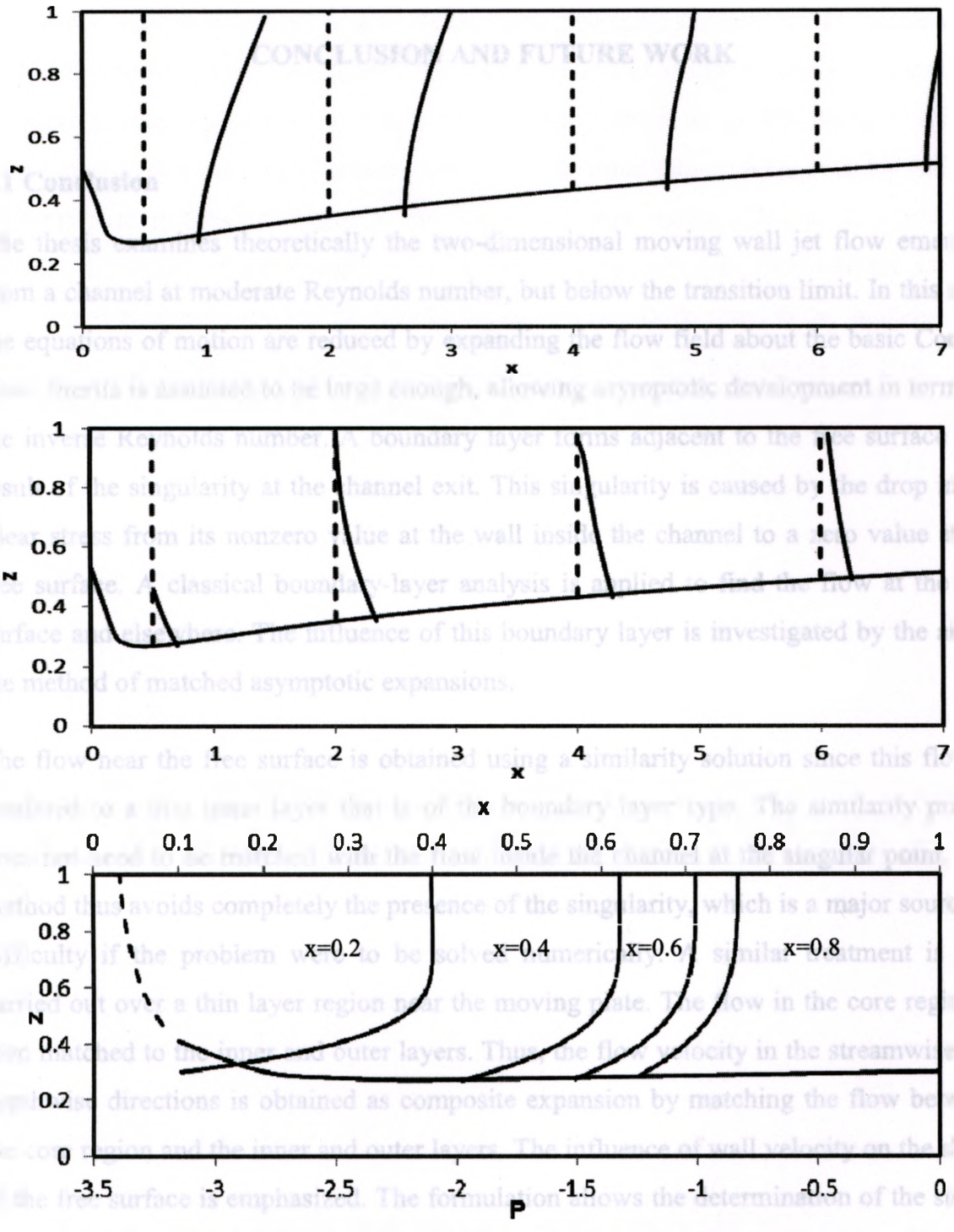

Figure 3.6: Variation of (a) streamwise velocity, (b) transverse velocity and (c) pressure profiles with position for ε = 0.3. Note: streamwise velocity and transverse velocity are drawn on same scale. The vertical dashed line is the origin at each position.

CHAPTER-4

CONCLUSION AND FUTURE WORK

4.1 Conclusion

The thesis examines theoretically the two-dimensional moving wall jet flow emerging from a channel at moderate Reynolds number, but below the transition limit. In this case, the equations of motion are reduced by expanding the flow field about the basic Couette flow. Inertia is assumed to be large enough, allowing asymptotic development in terms of the inverse Reynolds number. A boundary layer forms adjacent to the free surface as a result of the singularity at the channel exit. This singularity is caused by the drop in the shear stress from its nonzero value at the wall inside the channel to a zero value at the free surface. A classical boundary-layer analysis is applied to find the flow at the free surface and elsewhere. The influence of this boundary layer is investigated by the aid of the method of matched asymptotic expansions.

The flow near the free surface is obtained using a similarity solution since this flow is confined to a thin inner layer that is of the boundary layer type. The similarity profile does not need to be matched with the flow inside the channel at the singular point. The method thus avoids completely the presence of the singularity, which is a major source of difficulty if the problem were to be solved numerically. A similar treatment is also carried out over a thin layer region near the moving plate. The flow in the core region is then matched to the inner and outer layers. Thus, the flow velocity in the streamwise and depthwise directions is obtained as composite expansion by matching the flow between the core region and the inner and outer layers. The influence of wall velocity on the shape of the free surface is emphasized. The formulation allows the determination of the steady state flow and free surface profiles. It is found that the jet surface becomes singular very close to the exit. Thus the current method is not valid very close to the exit or very far downstream.

4.2 Future work

The method can thus be used to provide the correct boundary conditions to determine the jet development further downstream. The specification of adequate boundary conditions is often a major problem in this case. Another extension of the current work is axisymmetric flow exiting an annular tube, with the inner tube moving at some velocity. This problem is directly related to the process of wire coating. The work would thus provide the shape of the coating layer on the moving cylinder. Heat transfer aspects, which have been neglected in the present thesis, can be incorporated in the analysis. This is an important extension since cooling is often associated with the coating process.

REFERENCES

DENIER, J. P. & DABROWSKI, P. P. 2004 On the boundary-layer equations for power-law fluids. *Proc. R. Soc. Lond. A*, **460**, 3143.

GLAUERT, M. B. 1956 The wall jet. *J. Fluid Mech.* 1, 625.

GOREN, S. L. & WRONSKI, S. 1966 The shape of low-speed capillary jets of Newtonian liquids. *J. Fluid Mech.* **25**, 185.

HIGGINS, B. G. 1982 Downstream development of two-dimensional viscocapillary film flow. *Ind. Eng. Chem. Res.* **21**, 168.

MAGYARI, E. & WEIDMAN, P. D. 2006 Heat transfer characteristics of the alzebraically decaying Glauert jet. *Heat Mass Transfer.* **43**: 165-173.

MAHMOOD, T. 1986 A laminar wall jet on moving wall. *Acta Mechanica.* **71**: 51-60.

MAKI, H. 1983 Experimental studies on the combined flow filed formed by a moving wall and a wall jet running parallel to it. *Bullt. Japan Soc. Mech Eng.* **26**, 2100.

MIDDLEMAN, S. & GAVIS, J. 1961 Expansion and contraction of capillary jets of viscoelastic liquids. *Phys. Fluids.* **4**(8), 963.

MIDDLEMAN, S. 1978 High speed wire coating by withdrawal from a bath of viscoelastic liquid. *Polymer Engineering and Science.* Volume 18, No. 5.

MIYAKE, Y., MUKAI, E. & IEMOTO, Y. 1979 On a two-dimensional laminar liquid jet. *Bullt. Japan Soc. Mech. Eng.* **22**, 1382.

MITSOULIS, E. 1986 Finite element analysis of wire coating. *Polymer Engineering and Science.* Volume 18, No. 5.

MITSOULIS, E, WAGNER & HENG, F. L. 1988 Numerical simulation of wire-coating low-density polyethylene: theory and experiments.*Polymer Engineering and Science.* Volume 28, No. 5.

MITSOULIS, E, WAGNER & HENG, F. L. 1988 Numerical simulation of wire-coating low-density polyethylene: theory and experiments.*Polymer Engineering and Science.* Volume 28, No. 5.

PANTOKRATORAS, A. 2011. The nonsimilar laminar wall jet along a moving wall, in a free stream and in a free stream/moving wall. *Applied Mathematical Modelling.* **35**, 471-481.

PASQUALI, M. & SCRIVEN, L.E. 2002 Free surface flows of polymer solutions with models based on the conformation tensor, *J. Non-Newtonian Fluid Mech.* **108**, 363

PHILIPPE, C. & DUMARGUE, P. 1991 Étude de l'établissement d'un jet liquide laminaire émergeant d'une conduite cylindrique verticale semi-infinie et soumis à l'influence de la gravité. *J. Appl. Math. Phys.* (*ZAMP*) **42**, 227.

ROSS, A.B, WILSON, S.K. & DUFFY, B.R.. 1999 Blade coating of a power-law fluid. *Phys. Fluids.* Volume 11, No. 5.

RUSCHAK, K. J. & SCRIVEN, L. E. 1977 Developing flow on a vertical wall, *J. Fluid Mech.* **81**, 305.

SAKIADIS, B.C.. 1961 Boundary layer behaviour on continuous solid surface: ii. The boundary layer on a continuous flat surface. *A.I.Ch.E. Journal.* Vol. 7, No. 2.

SCHLICHTING, H., GERSTEN, K.. 2003. *Boundary Layer theory.*

SHI, J. M., BREUER, M. & DURST, F. 2004 A combined analytical–numerical method for treating corner singularities in viscous flow predictions. *Int. J. Num. Methods Fluids* **45**, 659

SMITH, F.T 1975 Flow through constricted or dilated pipes and channels: Part 1 *Q.Jl Mech. appl. Math.* **29**,343

SMITH, F.T 1975 Flow through constricted or dilated pipes and channels: Part 2 *Q.Jl Mech. appl. Math.* **29**,365

SMITH, F.T 1979 The separating flow through a severely constricted symmetric tube *J. Fluid Mech.* **90**,725

SOBEY, I. J. 2005 *Interactive boundary layer theory* (Oxford University Press, Oxford).

TSUKIJI, T. & TAKAHASHI, K. 1987 Numerical analysis of an axisymmetric jet using a streamline coordinate system. *JSME Int. J.* **30**, 1406.

VAN DYKE, M. D. 1964 *Perturbation Methods in Fluid Mechanics*. (Academic Press, New York)

WATSON, E. 1964 The spread of a liquid jet over a horizontal plane. *J. Fluid Mech.* **20**, 481.

WILSON, D. E. 1986 A similarity solution for axisymmetric viscous-gravity jet. *Phys. Fluids* **29**(3), 632.

ZHAO, J. & KHAYAT, R. E. 2007 Spread of non-Newtonian liquid jet over a horizontal plate. *J. Fluid Mech.* **613**, 411.

APPENDIX

Asymptotic solution of $f_2(\theta)$

In this appendix, we follow Tillett's (1968) approach to determine the asymptotic solution.

From the equation of $f_2(\theta)$ in (2.22),

$$f_2''' + \frac{2}{3} f_2 f_2'' - \frac{1}{3} f_2'^2 = 0 \tag{A1}$$

where the boundary conditions are,

$$f_2(0) = f_2''(0) = 0 \tag{A2}$$

Setting $t = \theta + c$, where c is arbitrary, and

$$f_2(t) = \alpha t^2 + g(t) \tag{A3}$$

where α is a constant. The function αt^2 satisfies (A1) but not the boundary condition. From (A3),

$$f_2' = 2\alpha t + g',\ f_2'' = 2\alpha + g'',\ f_2''' = g''' \tag{A4}$$

Substituting (A4) into (A1) we get

$$g''' + \frac{2}{3}\alpha t^2 g'' - \frac{4}{3}\alpha t g' + \frac{4}{3}\alpha g + \frac{2}{3} g g'' - \frac{1}{3} g'^2 = 0 \tag{A5}$$

Omitting the quadratic terms from (A5) we get,

$$g''' + \frac{2}{3}\alpha t^2 g'' - \frac{4}{3}\alpha t g' + \frac{4}{3}\alpha g = 0 \tag{A6}$$

Two solutions of (A5) are $g = t$ and $g = t^2$. To find a third, Tillett set $g(t) = th(t)$. Therefore,

$$g' = h + th',\ g'' = 2h' + th'',\ g''' = 3h'' + th''' \tag{A7}$$

Substituting (A7) into (A6) we get the following,

$$h''' + \left(3t^{-1} + \frac{2}{3}\alpha t^2\right)h'' = 0 \tag{A8}$$

Let, $P(t) = 3t^{-1} + \frac{2}{3}\alpha t^2$ and $h'' = f$. Therefore (A8) can be written as,

$$f' + P(t)f = 0 \tag{A9}$$

$$e^{\int_0^t P(t)dt} f' + P(t)e^{\int_0^t P(t)dt} f = 0 \tag{A10}$$

$$\frac{d}{dt}e^{\int_0^t P(t)dt} = e^{\int_0^t P(t)dt}\frac{d}{dt}\int P(t)dt = P(t)e^{\int_0^t P(t)dt} \text{[From Leibniz theorem]} \tag{A11}$$

Substituting (A11) in (A10) we achieve the following,

$$e^{\int_0^t P(t)dt} f' + \frac{d}{dt}e^{\int_0^t P(t)dt} = 0$$

$$\frac{d}{dt}\left[e^{\int_0^t P(t)dt} f\right] = 0 \tag{A12}$$

$$e^{\int_0^t P(t)dt} f = \text{constant}$$

$$f = Ce^{-\int_0^t P(t)dt} = h''$$

Then,

$$\int P(t)dt = \frac{2}{9}\alpha t^3 \tag{A13}$$

Therefore the general solution of (A6) becomes,

$$g(t) = At^2 + Bt + Ce^{-\frac{2}{9}\alpha t^3}\left\{\frac{81}{4\alpha^2 t^6} + o(t^{-6})\right\} = 0 \qquad \text{(A14)}$$

Taking A= B= 0, we get the asymptotic solution,

$$f_2(t) \sim \alpha t^2 + Ce^{-\frac{2}{9}\alpha t^3}\left\{\frac{81}{4\alpha^2 t^6} + \ldots\right\} \qquad \text{(A15)}$$